AD

USAAVLABS TECHNICAL REPORT 69-19

FEASIBILITY OF USING OPTICAL CORRELATION TECHNIQUE FOR DETECTING IMPENDING FATIGUE FAILURE

By

K. C. Chuang

E. Marom

April 1969

U. S. ARMY AVIATION MATERIEL LABORATORIES
FORT EUSTIS, VIRGINIA

CONTRACT DAAJ02-68-C-0024

BENDIX RESEARCH LABORATORIES

SOUTHFIELD, MICHIGAN

Disclaimers

The findings in this report are not to be construed as an official Department of the Army position unless so designated by other authorized documents.

When Government drawings, specifications, or other data are used for any purpose other than in connection with a definitely related Government procurement operation, the United States Government thereby incurs no responsibility nor any obligation whatsoever; and the fact that the Government may have formulated, furnished, or in any way supplied the said drawings, specifications, or other data is not to be regarded by implication or otherwise as in any manner licensing the holder or any other person or corporation, or conveying any rights or permission, to manufacture, use, or sell any patented invention that may in any way be related thereto.

Trade names cited in this report do not constitute an official endorsement or approval of the use of such commercial hardware or software.

Disposition Instructions

Destroy this report when no longer needed. Do not return it to the originator.

DEPARTMENT OF THE ARMY
U. S. ARMY AVIATION MATERIEL LABORATORIES
FORT EUSTIS, VIRGINIA 23604

The effort reported herein is a part of a program to develop concepts of aircraft maintenance, inspection, and diagnostic equipment suitable for field application. The report presents the results of the evaluation of an optical correlation technique as a candidate concept for detecting impending fatigue failure. The technique was successful in detecting early initiation of fatigue cracks.

This command concurs with the findings of the contractor.

Task 1F162203A43405
Contract DAAJ02-68-C-0024
USAAVLABS Technical Report 69-19
April 1969

FEASIBILITY OF USING OPTICAL CORRELATION TECHNIQUE FOR DETECTING IMPENDING FATIGUE FAILURE

Final Report

By

K. C. Chuang
E. Marom

Prepared by

Bendix Research Laboratories
Southfield, Michigan

for

U.S. ARMY AVIATION MATERIEL LABORATORIES
FORT EUSTIS, VIRGINIA

ABSTRACT

An investigation to determine the feasibility of using an optical correlation technique to detect fatigue cracks in materials is discussed. The optical system used included a helium-neon gas laser for generating coherent light, a commercially available photographic plate for recording the hologram, and a photomultiplier tube for measuring the light intensity. As a part of the investigation, holographic interferometric experiments were performed for comparison. During testing, aluminum-alloy specimens with various surface finishes and configurations were subjected to different stress levels and the effects were measured. Results indicated that the optical correlation technique is capable of detecting cracks as small as 0.05 mm in length and can detect even smaller dimensions in width and depth, although in practice 1 mm in length is the resolution limited by the instrumentation. In comparison, the resolution of the holographic interferometric technique was found to be limited to the width of the specimen, making it less sensitive in detecting surface deformation. The sensitivity of neither method was affected by surface finish, stress level, or specimen configuration.

TABLE OF CONTENTS

LIST OF ILLUSTRATIONS

BLANK PAGE

SECTION 1
INTRODUCTION

1.1 FATIGUE FAILURE

Despite a large number of investigations in past years, fatigue remains the most common cause of service failure in components as well as in structures. Localized instabilities or changes in the microstructure of a material during repeated stressing result in a "history" effect that makes it impossible to predict fatigue life by equation-of-state methods. Furthermore, because the microstructures of most engineering materials are not homogeneous, and because well-established statistical data are not available for a given material, it is essential to treat each specimen independently. Therefore, only a sensitive inspection method to detect or evaluate fatigue can really prevent a catastrophic failure.

The development of fatigue failure is generally divided into two categories: crack nucleation and crack propagation. Although the dividing line between these processes is not clear-cut, the critical flaw size for propagation to occur is considered to be the same as the average spacing between dislocated cell walls ($\approx 2\mu$ in aluminum at room temperature). Regarding the inception of crack nucleation, several dislocation mechanisms have been postulated. These mechanisms include the formation of slip bands (the cause of intrusions (notches) and extrusions), the development of dislocation cross-slip, and the formation of pores by vacancy clustering.

Once a crack forms, it has to propagate into a work-hardened lattice region. The propagation proceeds only when conditions are such that the energy supplied at the crack's tip by the stress exceeds the elastic energy stored in the lattice, the plastic energy required to deform the lattice, and the surface energy required to extend the crack. The process depends on the material's history and temperature, as well as the amplitude of the stress. A material may thus contain many subcritical cracks and yet not fail in fracture. To determine whether a structure is approaching its fatigue limit, the flaw sizes and the rates of crack propagation under service conditions must be known.

In most engineering materials, cracks often propagate from existing structural singularities such as voids, inclusions, and regions of high residual stress. Because of this, most of these materials do not pass through the crack nucleation phase before failure occurs.

1.2 PURPOSE OF THIS INVESTIGATION

Many techniques have been developed in recent years to detect incipient fatigue failure. Thermal, mechanical, electrical, and acoustical methods have been extensively explored. Although some of these techniques have been useful for specific applications, there are always limitations to their being used in general inspection. The development of the laser, however, with characteristics of monochromaticity, coherency, and intensity, has opened up a number of highly sensitive optical techniques for detecting incipient fatigue failure in different materials.

The activities at Bendix Research Laboratories have resulted in the development of an optical correlation technique that appears to be promising for quantitatively evaluating fatigue-induced damage. The purpose of the investigation discussed herein was to determine the feasibility of using this optical correlation technique to detect fatigue damage and to compare the technique with holographic interferometry, currently the most commonly used coherent optical inspection technique.

1.3 OPTICAL CORRELATION TECHNIQUE

The optical correlation technique employs a matched filter to measure the resemblance between the surface structures of a stressed and an unstressed area. If f_o is a function that describes the surface of a given area, A, at time zero, and if f_k describes the surface at a later time, k, the cross-correlation function, C_{ok}, is defined as

$$C_{ok}(\xi,\eta) = \iint_A f_o(x,y)\, f_k(x-\xi,\, y-\eta)\, dx\, dy$$

This function can be measured optically by a system first described by Vander Lugt.* The basis for optical correlation techniques is as follows:

(1) The light distribution in the rear focal plane of a spherical lens is related to the wave front input in its front focal plane by a Fourier transformation.

(2) A holographic recording preserves both the amplitude and the phase information of a wave front.

A Fourier-transform hologram is used as a matched filter for optical correlation. Although the optical correlation technique is not particularly sensitive to uniform elastic strain in pure tension and compression, most materials are known to deform nonuniformly, even at a stress considerably smaller than the flaw stress. When local deformation occurs, the correlation function decreases rapidly with increased

*A. Vander Lugt, SIGNAL DETECTION BY COMPLEX SPATIAL FILTERING, IEEE Transactions on Information Theory, IT-10, April 1964, 139-145

deformation. This is the major advantage that the optical correlation technique has over other strain-monitoring methods for detecting surface deformation caused by repeated stressing in fatigue. Since the surface structure is utilized for making the Fourier hologram, no particular surface preparation is necessary. In fact, it is desirable to have the surface in an "as-machined" condition.

When a crack grows in excess of the critical dimensions, it causes relative movement and distortion of the two portions of material that it separates. When this occurs, only part of the area can be correlated, regardless of how the matched filter is adjusted to compensate for the deformation of the specimen. This characteristic contributes to the extreme sensitivity of the correlation technique in the detection of incipient cracks. In principle, changes on the order of 1 micron in surface structure can be detected.

1.4 HOLOGRAPHIC INTERFEROMETRY

Holographic interferometry is gaining popularity as an important nondestructive testing technique. This technique utilizes the property of a hologram to reconstruct a virtual image at the position of the original object. A hologram of an object is first exposed, developed, and then placed back in the exact position in which it was exposed. When the object is subsequently subjected to stress, the resulting surface distortion changes the phase of the reflected light, which interferes with the light field reconstructed from the hologram. Interference fringes can then be observed.

Since the interference fringes show the contour of the equal normal displacement of the two wave fronts in increments of half a wavelength, their pattern reveals a general deformation. In addition, the observed fringe pattern can be further analyzed to obtain local strain. If the structure contains a flaw, the fringe pattern at the surface over the flaw appears to be different to the point that sometimes even a discontinuity can be observed. However, for the purpose of nondestructive inspection, it is not necessary to analyze for strain. A simple comparison with a pattern obtained from a flawless structure should be sufficient to reveal whether the flaw is in excess of certain dimensions. Since a hologram records three-dimensional images, this technique is applicable to any design and to any moderately reflective surface.

1.5 SCOPE OF THE WORK

The program was conducted with a one-man-year effort at the Solid State and Thin Film Department of the Bendix Research Laboratories. The following work was performed:

(1) Correlation measurements on 10 specimens and holographic interferometry on 10 specimens of 2024 aluminum alloy, subjected to strain cycling at $\pm 3 \times 10^{-3}$ strain amplitude.

(2) Investigation of the effects of stress levels and surface finish on the characteristics of the curves obtained by plotting correlation intensity against the number of strain cycles. The results were then analyzed to demonstrate the reproducibility of the method (two specimens were used for two stress levels and for two surface finishes).

(3) Establishment of a comprehensive, standard method for plotting the data. This was done concurrently with the experiments run in item (1). Also, additional measurements were made to collect data for different kinds of plotting methods.

(4) Comparison of optical correlation measurement results with electron microscopy and metallographic observation of three specimens (performed concurrently with the experiments run in item (1)).

(5) Development of techniques to make optical correlation measurements on large and nonplanar surfaces.

(6) Conception of a prototype instrument for fatigue detection.

SECTION 2

EXPERIMENTAL METHODS

2.1 MATERIALS AND SPECIMEN PREPARATION

Specimens were prepared from 0.065-inch-thick commercial sheet stock of 2024 (T3) and 2024 (T4) aluminum alloys. The sheets were cut and milled with standard shop procedure. Two specimen configurations were chosen: a T-shaped slab for stress gradient studies and a tapered slab for uniform stress distribution studies. A photograph of the specimens is shown in Figure 1. Some specimens were tested as received (in the as-rolled condition), some were tested after being sandblasted, some were tested after being finished with No. 600 emery paper, and some were tested after being chemically brightened or polished.

2.2 EXPERIMENTAL SETUP

2.2.1 Strain Cycling

A schematic diagram of the setup used for strain cycling is shown in Figure 2. In this setup, a permanent magnetic disc was attached to the free end of the cantilever-mounted aluminum specimen. The magnet, and hence the specimen, was actuated with an electromagnet driven by an audio amplifier. The vibrational frequency was tuned to the resonance frequency of the specimen-magnet, and the vibrational amplitude was measured from a distance with a vernier-telescope. The strain amplitude was calculated from the harmonic vibration equation and was calibrated with a strain gauge pasted on the specimen's surface. The number of strain cycles was counted with an electronic counter. Occasionally, it was necessary to adjust the frequency to maintain resonance. The strain cycling was discontinued when a crack was observed with 200X microscopic inspection or when the correlation intensity decreased to less than 20 percent of its initial value.

2.2.2 Optical System

The experimental setup used for optical correlation measurements and holographic interferometry is shown schematically in Figure 3 and photographically in Figure 4. A helium-neon gas laser was used to provide a coherent light, photographic plates were used for recording the Fourier-transform hologram, and a photomultiplier tube, mounted on a micropositioner, was used for measuring the light intensity. The photomultiplier was connected to a high-precision volt-ammeter and then to a digital voltmeter for reading.

The laser light was split into two beam paths, one of which was incident to the specimen. Each beam was collimated with a 25X objective lens and a 10μ pinhole. The beam incident to the specimen was designated as the signal beam, since it carried the information

of the surface detail. The other beam was called the reference beam, because it was used only for recording the hologram. The path lengths of these two beams were equalized to within 1 cm, and the angle between these beams incident at the photographic plate was approximately 22 degrees. The intensity of the reference beam was twice that of the signal beam at the photographic plate. A pair of f:3.5, 18-cm corrected lenses were used as the transform lens and the relay lens. The photographic plate was located at the rear focal plane of the transform lens via reflection from the specimen. The specimen-to-hologram plate distance was approximately 10 cm and the diameter of the reference beam was 5 cm. The Fourier hologram thus contained frequencies up to approximately 400 mm^{-1}.

The photographic plate was held with three-point contact registration pins on a micropositioner. After proper exposure, the plate was removed from its holder, processed in a darkroom, and then placed back in the plate holder to serve as a matched filter. The reference beam was then blocked. If the filter position is correct (defined here as that position which results in the maximum correlation intensity), the correlation display can be observed in the back focal plane of the relay lens. Due to a slight distortion and possible shrinkage in the emulsion of the photographic plate, however, it was necessary to adjust the filter position. After this adjustment was made, the correlation intensity was measured with a photomultiplier. To ensure maximum efficiency, a 0.3-mm-diameter pinhole was placed before the photomultiplier tube to allow only the center of the correlation display to get through. The half-width of the correlation peak was approximately 20μ.

To achieve linearity, it was necessary to make sure that the light intensity did not exceed the saturation level of the photocathode. For this setup, the saturation output current reading was approximately 500 μA.

2.2.3 Holographic Interferometry

The procedure used for holographic interferometry was the same as that used for the optical correlation measurements, except that observation was made from behind the hologram without the relay lens. A 35-mm camera was used to record the interference pattern. To obtain a strong fringe contrast, a neutral density filter was used to attenuate the signal beam.

SECTION 3
RESULTS

3.1 REPRODUCIBILITY TESTS

The correlation intensities measured in a number of aluminum alloy specimens subjected to a constant cyclic strain amplitude of about $\pm 3.4 \times 10^{-3}$ are shown in Figures 5, 6, 7, and 8. Figure 5 shows a plot of the normalized correlation intensity versus run time (nominally 182 ±2 cycles per second) for specimens having a longitudinal texture in the as-received (as-rolled) condition. Figures 6 and 7 show the test results for specimens with the same texture but finished with No. 600 emery paper. Figure 8 shows the test results for specimens having a transverse texture in the as-rolled surface condition. The specimens in the as-rolled condition appeared to have shorter fatigue life than those finished with emery paper.

Although there is considerable variation in the lives of the specimens within a group of specimens, all of these curves show that correlation intensity decreases in three stages. The first decrease, Stage I, occurs within a few thousand strain cycles (≈10 seconds of run time); the second decrease, Stage II, extends from a few thousand cycles to a few million cycles (usually more than 60 minutes of run time); the third decrease, Stage III, ranges from 10^5 cycles to a few million cycles (15 minutes of run time on the average). The difference in fatigue life appears to be determined, mainly, by Stage II. During Stage III, a crack about 1 mm in length would usually be detected when the correlation intensity decreased to less than 50 percent of the value it had at the outset of this stage.

These results suggest that the correlation intensity provides a good measure of surface deformation and that the decrease during the third stage reflects crack propagation. Although no two specimens deform identically, the degree of damage induced by strain cycling is well represented by a decrease in the correlation intensity.

3.1.1 Detection of Incipient Crack Propagation

A number of specimens were tested until separation into two pieces occurred. The number of stress cycles endured by some specimens prior to incipient crack propagation, as reflected by correlation intensity measurements and the number of stress cycles following incipient failure, are tabulated as follows:

Specimen	Surface Finish	Nucleation Cycles	Stress Cycles After Incipient Failure
N7	No. 600 Emery Paper (Random Scratches)	2.21×10^6	4.75×10^5
N9	No. 600 Emery Paper (Random Scratches)	2.81×10^6	6.87×10^5
N10	As Rolled	6.99×10^5	3.46×10^5
N11	As Rolled	5.4×10^5	5.08×10^5

It is noted that while the nucleation period varied from specimen to specimen, nearly all specimens endured about the same number of strain cycles after incipient failure. It is expected that a specimen tested at a low strain amplitude would have a high ratio of nucleation-to-crack propagation cycles. This indicates that the life of a specimen after the outset of crack propagation may be predicted on the basis of correlation intensity measurements.

On the basis of the four samples mentioned above, the accuracy in predicting a failure will now be evaluated.

Assuming that the number of stress cycles leading to complete failure after nucleation is 3×10^5 (slightly lower than the smallest value for the four specimens), the ratio of the predicted stress cycles to the stress cycles to failure may be defined as a measure of accuracy and dependability. Thus, in mathematical terms

$$Q = \frac{C \text{ predicted}}{C \text{ failure}} = \frac{C \text{ nucleation} + 3 \times 10^5}{C \text{ nucleation} + C \text{ leading to failure}}$$

For the four samples that are being compared here, the above equation will lead to the following ratios:

For Specimen N7 $\quad Q = \frac{2.51}{2.685} = 0.935$

For Specimen N9 $\quad Q = \frac{3.11}{3.497} = 0.89$

For Specimen N10 $\quad Q = \frac{9.99}{1.045} = 0.955$

For Specimen N11 $\quad Q = \frac{8.4}{10.46} = 0.80$

These data are not sufficient to draw more general conclusions. Of course, Q>1 will mean a catastrophic failure where the specimen fails before the predicted time. The probability of such occurrence, however, is undetermined. A systematic study of various stress cycles for various components are needed for this determination.

3.2 EFFECTS OF STRESS LEVEL ON FATIGUE LIFE

The effects of stress level on fatigue life are indicated by the test results shown in Figure 9. The normalized correlation intensity was plotted against the logarithm of the run time. The specimen subjected to the largest stress (strain amplitude) had the shortest life, as expected.

Stage I decreases occurred within 1000 cycles, regardless of the stress levels. The second stage was shortest for the specimen subjected to the largest strain. In Stage III, slope variations were observed in the curve representing the specimens subjected to strain of less than $\pm 3.4 \times 10^{-3}$, suggesting that crack propagation was not continuous in these specimens. The fractional correlation intensity remaining at the outset of Stage III tends to be larger, the smaller the strain amplitude.

The effects of the stress level on the decrease in the correlation intensity in Stage III are shown in Figure 10. A specimen was first subjected to a constant strain amplitude of $\pm 3.4 \times 10^{-3}$ for 300 minutes, then to cyclic strain amplitudes of $\pm 1.1 \times 10^{-3}$, $\pm 1.6 \times 10^{-3}$, $\pm 2.2 \times 10^{-3}$, $\pm 2.8 \times 10^{-3}$, and $\pm 3.4 \times 10^{-3}$. It was found that the rate of loss in correlation intensity is proportional to the increase in the stress level. This result was expected because cracks propagate faster as larger stresses are applied. It is noteworthy that at the beginning of Stage III (e.g., between 350 and 388 minutes), the correlation intensity remained constant when the strain amplitude was less than 1.6×10^{-6}. This suggests that for a given crack size, there is a critical stress level below which the crack will not propagate; thus, the correlation intensity does not change. As the crack grows larger, the critical stress becomes smaller. These results demonstrate the usefulness of the correlation technique in investigating crack propagation.

3.3 EFFECTS OF SURFACE FINISH ON OPTICAL CORRELATION

Specimens with polished, as-rolled, emery-paper-sanded, and chemically brightened surfaces were compared. The fatigue life of the as-rolled specimens appeared to be shortest, whereas mechanically polished specimens exhibited the longest life. Chemical treatment also tended to shorten the fatigue life. The Fourier-transform spectra of polished surfaces had high densities near the center (low-frequency location), while the spectra of the roughened surfaces appeared to be more uniformly distributed. (See Figure 11.) However, the different surface conditions did not seem to affect optical correlation. For example, Figure 12 shows the correlation intensity obtained alternatively from the polished face and the roughened face of a specimen. There is no obvious discontinuity between the segments representing the two surface conditions.

In preparing the matched filter for highly polished surfaces, it is necessary to select an optimum photographic process to obtain a strong correlation intensity. If necessary, the matched filter can be bleached after being developed to decrease the density near the center.

In general, specimens with roughened surfaces are easier to work with than as-rolled specimens because their spectra are more uniformly distributed. (The process parameters for a specimen with a uniform spectrum are not critical, and a good correlation display is easily achieved.) In view of this, it is desirable to have specimens with a certain surface roughness which is on the order of the wavelength of the coherent light source used. The as-machined surface is well suited for this reason.

3.4 METALLOGRAPHIC EXAMINATION

3.4.1 Optical Microscopy

All specimens were examined metallographically to relate surface deformation to loss in correlation. In general, however, the changes were so minute that the metallographic examination could reveal only large cracks. Typical changes in crack length due to additional strain cycles are shown in Figures 13 through 16. As can be noted, cracks started from the edge of those specimens finished with emery paper (Figures 13 and 14), whereas cracks started from the interior of those specimens with polished surfaces (Figures 15 and 16).

The lengths of three of the cracks determined from these metallographs are given in Figure 17 to show their relationship to the correlation intensity. Although a quantitative relationship appears to exist between the correlation intensity and the crack length for each specimen, a common relationship could not be established for all specimens. As shown in Figure 17, the annealed specimen, A5, exhibited more loss in correlation intensity than did the roughened (T3 rolled) specimens for a given crack length. Nevertheless, correlation intensity could be used as a measure of fatigue damage if all the specimens were nearly identical. At any rate, however, additional data are needed for statistical analyses before a quantitative relationship between the correlation intensity and crack dimensions can be established.

It must be noted that the crack length, as observed from metallographic examination, is not a representative measure of fatigue damage. In fact, the loss in correlation might be considered to be a more representative means of quantitatively evaluating fatigue damage since it provides a continuous measure.

Typical failure modes of specimens are shown in Figure 18. Failure usually occurs at the zone of maximum stress, as would be expected. A crack is generally propagated lengthwise a distance of one-half the specimen width before it penetrates through the thickness of the specimen.

3.4.2 X-Ray Diffraction

Some specimens were examined with X-ray Laue back diffraction. Typical diffraction patterns of a critical area before and after strain cycling are shown in Figure 19. Since the specimen is a polycrystalline alloy, the rings are neither continuous nor symmetric, as would be expected from powder or single-crystal specimens. Nevertheless, there are indications that strain cycling increases the misorientation between neighboring subgrains and thus increases the number of detectable diffraction spots.

3.4.3 Electron Microscopy

Although some electron micrographs were made of the specimens, the frame of this work did not provide sufficient funding for observing significant surface changes with electron microscopy. As a result, no firm conclusion can be drawn as to whether this method is in fact a suitable means for relating surface deformation with the loss in correlation.

3.5 SELECTIVE MASKING

3.5.1 Selective Masking of Matched Filters

Three tests were conducted to investigate the effects of selectively masking matched filters. The results obtained are shown in Figures 20 through 22. Blocking the high spatial frequency (outer spectrum) with a circular disc appeared to increase the sensitivity of detecting the beginning of Stage I, but it appeared to decrease the sensitivity of detecting the propagation of cracks in Stage III. Using a horizontal slit mask resulted in some improvement in sensitivity during Stage III, whereas using a vertical slit mask decreased the sensitivity. In general, the gain or loss in sensitivity due to masking is not pronounced; for all practical purposes, the masking of matched filters should not be necessary.

3.5.2 Selective Masking of the Specimen

Two correlation measurements were conducted to investigate the effects of selectively masking the specimen. The results are shown in Figure 23. As indicated in the figure, the correlation intensity of the four areas decreased in the order of 1, 2, 3, 4, suggesting that the largest crack should be in area No. 1. Metallographic examination confirmed this prediction. This technique is considered to be useful for locating cracks in a relatively large area.

3.6 LARGE-AREA CORRELATION

The feasibility of using multiple-beam correlation techniques to investigate relatively large areas was also studied. The procedure consisted of simultaneously illuminating two 1/2-inch-diameter circular

areas, 1 inch apart. Figure 24 shows the correlation intensities of the two spots plotted against strain. Making a hologram with the two areas illuminated simultaneously allows both areas to be correlated in a single correlation display. Such a technique could be used to detect deformations inside any area so illuminated.

3.7 CONCEPTION OF PROTOTYPE FIELD INSPECTION INSTRUMENT

A schematic of the design concept of a prototype field inspection instrument is shown in Figure 25. The laser, the collimators, the lenses, the photographic plate holder, and the photodetector will be mounted on a cast iron optical bench. Although some refinement of the optical system might be necessary, the most important factor is considered to be the support of the optical bench. To ensure stability, the bench will be supported pneumatically on a sliding platform which can be moved up or down on a vertical stand. In addition, the stand will be mounted on hydraulic vibration isolators, and the cart for carrying the stand will be bolted to the ground. A hydraulic jack will be used to lift the subject to be inspected, and a pneumatic actuator will be used to stress or vibrate the subject.

3.8 HOLOGRAPHIC INTERFEROMETRY

Typical holographic interferometry results are shown in Figures 26 through 29. The images in Figure 26 were obtained by double-exposing the holograms. The specimens were first strained at an amplitude of $\pm 3 \times 10^{-3}$ approximately 2000 times between exposures. As can be observed, the resulting interferograms exhibit strain patterns, indicating some bending in the specimens. The bending of the top fringes suggests that two cracks are propagating inward from the edges. Real-time observations were made by recording the results with a 35-mm camera, as shown in Figures 27 through 29. The fringe patterns in Figure 27 indicate the bending strain in the specimen, and Figure 29 shows patterns which suggest that a crack is forming at the lower left corner of the illuminated area. As predicted, a crack occurred; as the crack propagated, the number of fringes increased. The fringe pattern shown in Figure 29f corresponds to a crack length of approximately 2 mm. The results of simultaneous correlation measurements and interferometric observations are shown in Figure 30.

SECTION 4

DISCUSSION

4.1 OPTICAL CORRELATION AS A DETECTION TECHNIQUE FOR IMPENDING FATIGUE FAILURE

Experimental results obtained during the investigation have shown that the optical correlation technique can be used to detect incipient fatigue failure. In normal fatigue tests, the correlation intensity decreases very rapidly during the first few thousand strain cycles, but this change is primarily representative of the work hardening occurring in the metal. After the initial decrease, the correlation intensity remains nearly constant for a considerable number of strain cycles until the formation of incipient cracks occurs. This period corresponds to saturation hardening and is considered to be the incubation period for crack nucleation. Once a crack exceeds the critical limit, it begins to propagate with each additional strain cycle, causing the correlation intensity to decrease continuously. It is essential in investigating fatigue to differentiate between the decrease in correlation intensity occurring in Stage I and that occurring in State III. Fortunately, Stage I lasts only a few thousand cycles at most, and the decrease in correlation intensity seldom exceeds 50 percent. If a material does not contain cracks in excess of the critical size, the correlation intensity reaches a steady-state condition after a few thousand strain cycles. If the correlation intensity begins to decrease again after only a few additional strain cycles, one can be certain that it will continue to decrease until complete failure occurs. Repeated tests showed that a 50-percent decrease in correlation intensity from its value at the outset of Stage III normally indicates the occurrence of a crack on the order of 1 mm in length.

Since no two specimens deform in an identical manner, it was not possible to establish a quantitative relationship between correlation intensity and crack size. However, the flaw size appears to be inversely proportional to the logarithm of the correlation intensity of a given specimen.

4.2 EFFECTS OF STRESS LEVEL AND SURFACE FINISH ON THE DETECTION TECHNIQUE

The roughness of the surface finish tends to decrease the fatigue life of a material in a manner similar to that produced by raising the stress level. However these variables do not affect the application of the optical correlation technique for detecting incipient failures. In other words, a 50-percent decrease in correlation intensity during Stage III would indicate the occurrence of a flaw about 1 mm in length regardless of the stress level or surface finish.

4.3 PROCEDURE FOR INSPECTION

It follows from the preceding discussion that a standard procedure must be established to utilize the optical correlation technique for detecting incipient fatigue failures. Although an optimum procedure can be established to suit each particular application, the following requirements are considered to be essential for all applications:

(1) The optical system should be mechanically rigid and optically stable.*

(2) The illuminated area must contain the crack of interest.

(3) The laser output should be constant within the period of examination.

(4) The specimens need to be strain cycled with a reproducible loading pattern for a certain number of cycles.

(5) The test environment must be such that surface structure variation due to environment is negligible in comparison with deformation caused by the strain cycles alone.

A granite-top table is sufficiently stable for laboratory use. However, an industrial environment would require the use of a pneumatically suspended cast iron table to avoid vibrations. A continuous-wave laser of reasonable quality should be used to provide the coherent light, and the hologram should be recorded on a photographic plate. Other good-quality recording media having high resolution and stability of emulsion can also be considered; however, presently available photochromic materials are not suitable for this purpose. The photographic plate can be developed in situ. If the plate must be removed from its holder to be developed, the plate holder must be constructed so that the plate can be reinserted in its original position. After the hologram has been positioned to obtain maximum correlation intensity, the specimen can be subjected to a certain number of strain cycles.

Although dynamic measurements could be accomplished by using more complex instrumentation, the best results are obtained when the specimen remains static. The correlation intensity should be plotted on semilog paper against run time (or the number of strain cycles). Strain cycling should be continued until the correlation intensity reaches a constant value. Should the correlation intensity continue to decrease, strain cycling should be continued until the correlation intensity is less than 10 percent of its initial value. When this happens, the specimen should be considered as fatigued and put out of service.

---

*Although it is implied here that calibration of the equipment may be required, this is not the case since all correlation results are relative quantities. However, the filter position must be adjusted for maximum reading of the correlation intensity.

4.4 HOLOGRAPHIC INTERFEROMETRY

The requirements for holographic interferometry are the same as those for optical correlation. However, the former technique is not as sensitive as the optical correlation technique. The minimum crack length detectable using holographic interferometry is approximately the same as the thickness of the specimen (about 1.65 mm for these investigations). This technique does, however, offer some advantages over the optical correlation technique for field applications.

Since the coherent light source is used only during the time required for exposure, a high-energy pulse laser can be used. In addition, there is considerably less restriction upon the optics. Also, stress can be induced by heat as well as by a mechanical force.

The following procedures are applicable for inspection purposes:

(1) Double-exposed hologram. A double-exposed hologram (one exposure is made before stressing and another one after stressing) can be made which, when illuminated with the reference beam, will reveal a fringe pattern indicating the distortions in the object. Irregularity and discontinuity in the fringe pattern indicate stress-concentrating singularities. The pattern can also be compared to a pattern obtained from a sound specimen to detect flaws and cracks. Although the specimen is not observed in real-time, a permanent record is obtained that can be preserved for subsequent comparison.

(2) Time-exposed hologram. If the specimen is subjected to constant vibrational stresses, the holographic plate can be exposed for a short time while the specimen is vibrating. The nodes and antinodes of the vibrating specimen generate fringe patterns in the reconstructed image. Hence, a change in the fringe pattern indicates the presence of flaws. This method is applicable, however, only to small constant amplitude harmonic vibrations. For complex vibrations, the exposure time must be shortened so that it does not exceed the period in which the vibrational pattern of the specimen remains constant.

(3) Real-time observation in holographic interferometry. If the hologram of an unstressed specimen is illuminated with the original beams to reconstruct a virtual image superimposed on the object itself, one can observe in real-time the formation and the change in the fringe pattern when the specimen is stressed. The fringe pattern forms whenever the phase of the reconstructed wave front differs from the wave front reflected from the specimen's surface. If the specimen remains rigid, the fringe pattern is observed at the surface of the specimen. Usually a small displacement is unavoidable, and the fringe pattern does not fall on the plane of the specimen. Care must

be taken in interpreting the fringe pattern. In most cases, the strain effects can only be induced from analyses of the fringe pattern. For inspection purposes, irregularity and discontinuity in the fringe pattern are more important than the configuration of the fringe pattern itself.

SECTION 5

SUMMARY AND CONCLUSIONS

The results of this investigation demonstrate the feasibility of using the optical correlation technique to detect incipient fatigue failure. The method is applicable to any diffusely reflective surface; the crystalline structure and the surface finish are immaterial. Minute changes in surface topography, particularly relative movements of one portion of a surface with respect to another portion, cause a drastic decrease in the correlation intensity. Since this technique detects changes in a surface due to cracks rather than the existence of cracks themselves, it is necessary to subject the specimen to be inspected to a slight strain. If the specimen contains a crack or flaw, it will be slightly deformed even after the strain is discontinued. Deformation causes a decrease in the correlation intensity and thus is easily detected. This technique is capable of detecting cracks as small as 0.05 mm in length and can detect even smaller dimensions in depth and width, although in practice 1 mm in length is the resolution limited by the instrumentation. The optical correlation technique is more sensitive in detecting surface distortion than the holographic interferometric technique, which has a resolution limit approximately equal to the thickness of the specimen. However, both methods are capable of detecting subsurface cracks as well as surface cracks. The sensitivities of both techniques are not affected by surface finish, stress level, or configuration of the specimens. A major difference between the two approaches is that optical correlation requires an extremely stable coherent light source, whereas holographic interferometry allows certain fluctuations in the intensity of the source. In addition, the optical correlation method gives a quantitative measure of the damage and thus requires no judgment of the operator, whereas the holographic interferometric approach requires a trained technician to interpret the results.

As in all holographic work, the optical correlation method requires measurement to be made after adjusting the photographic plate position. This means that fine mechanical positioning devices are needed to allow for optimum placement of the filter (photographic plate). Since the measurement obtained in this fashion is always related to the original measurement made right after the filter has been exposed and developed, there is no need of calibrating the setup.

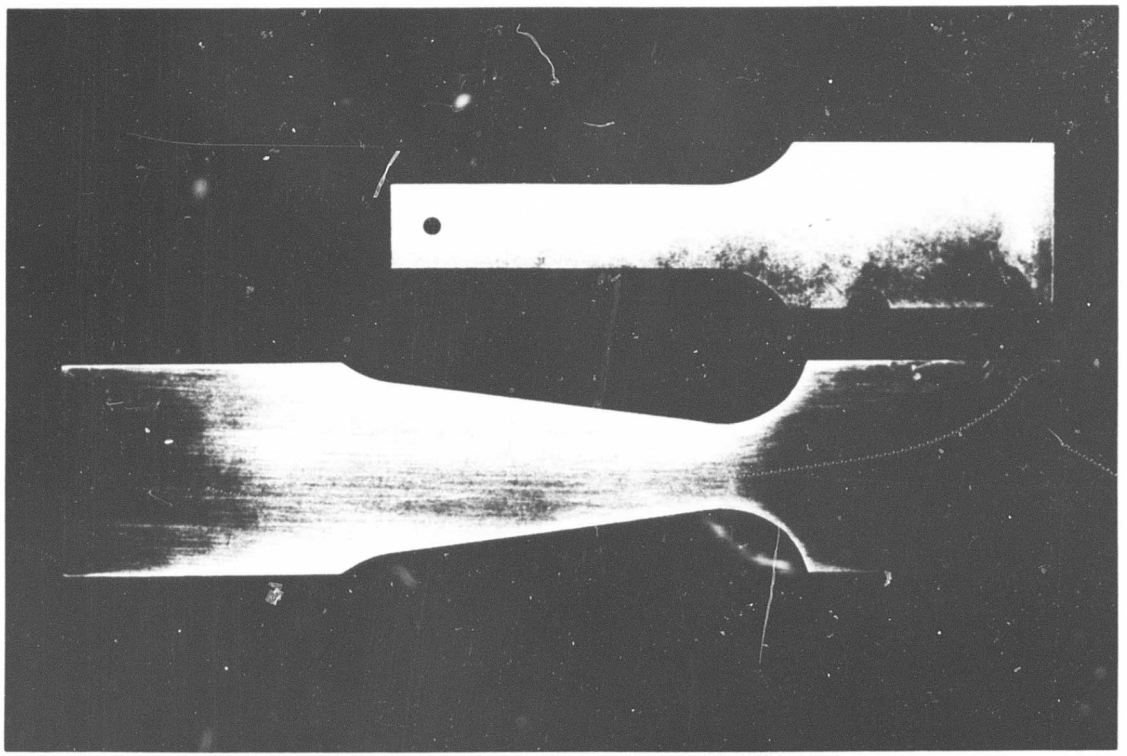

Figure 1. Photographs of the Specimens.

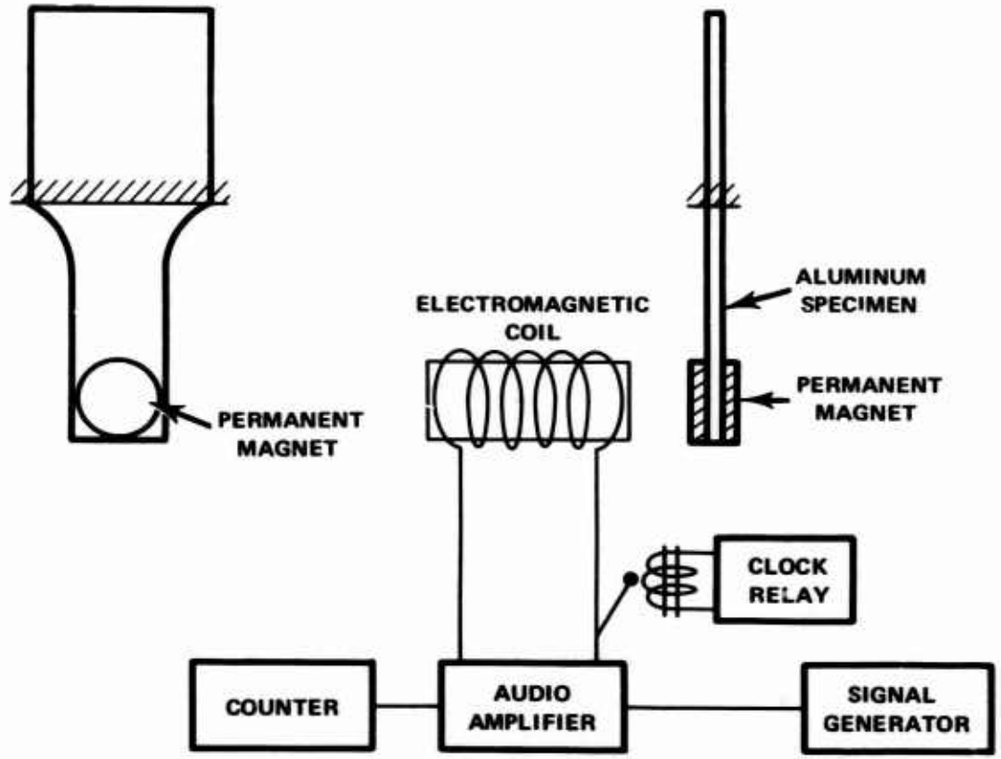

Figure 2. Schematic Diagram of the Experimental Setup for Strain Cycling.

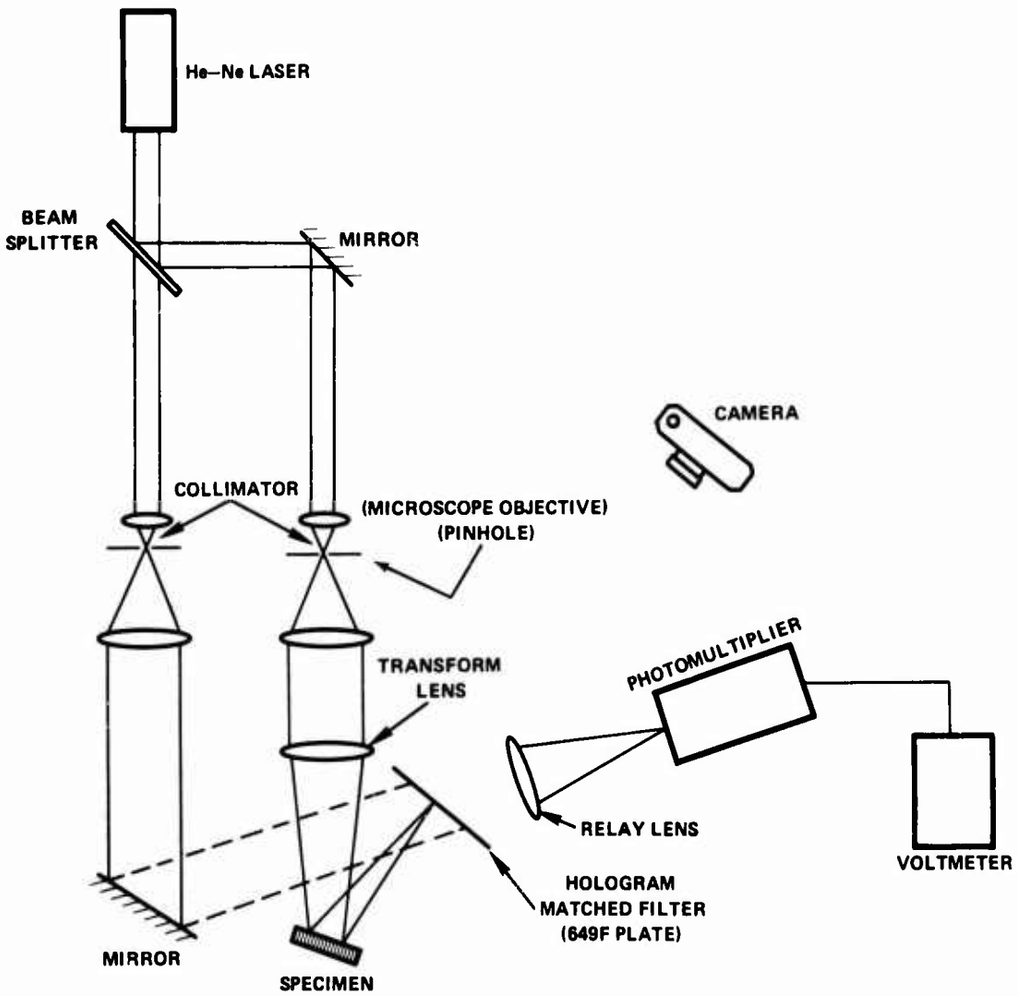

Figure 3. Schematic Diagram of Experimental Setup for Optical Correlation and Holographic Interferometry.

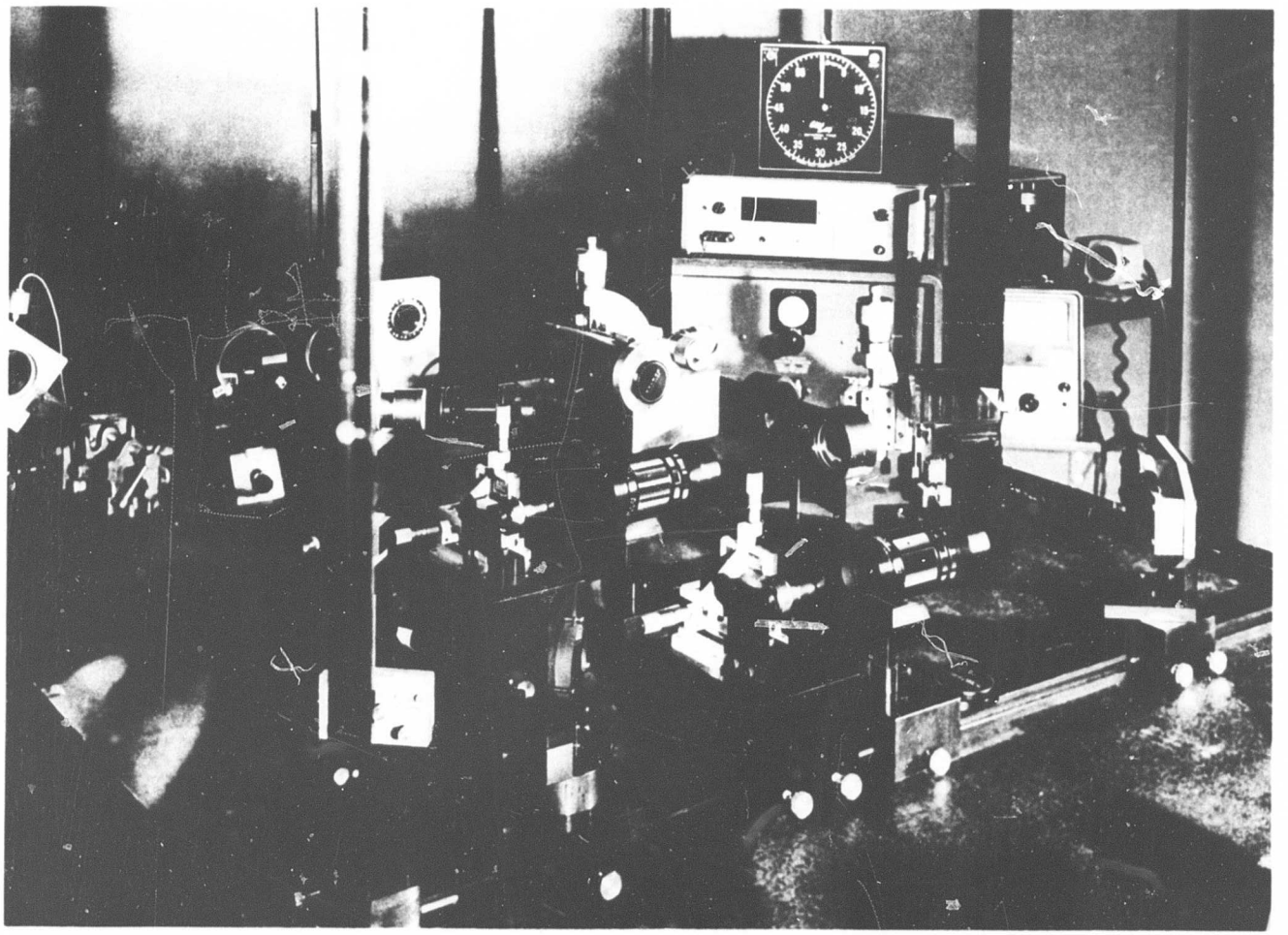

Figure 4. Photograph of Experimental Setup for Optical Correlation and Holographic Interferometry.

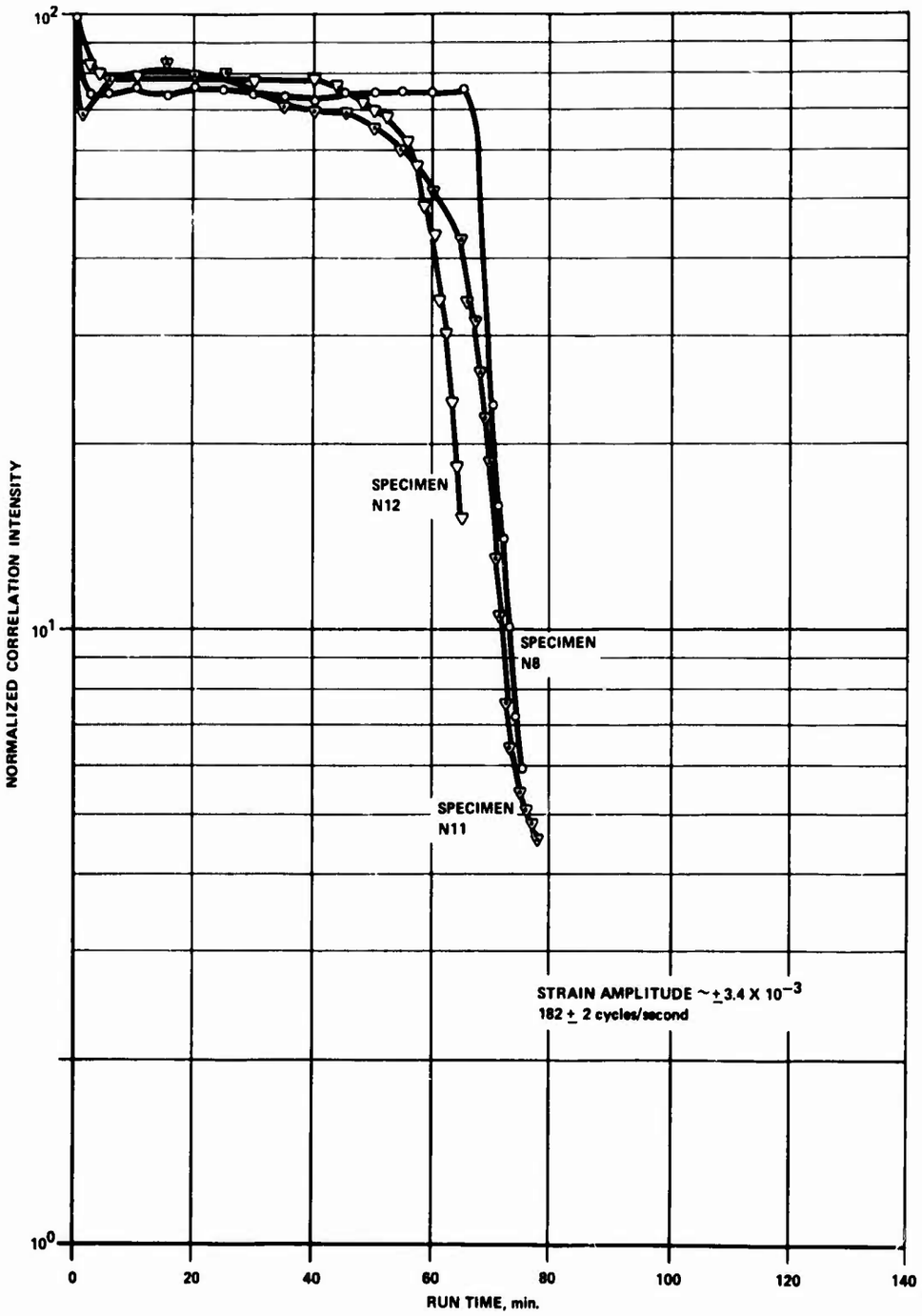

Figure 5. Correlation Intensity Versus Run Time for Specimens With Longitudinal Texture (As-Rolled Surfaces).

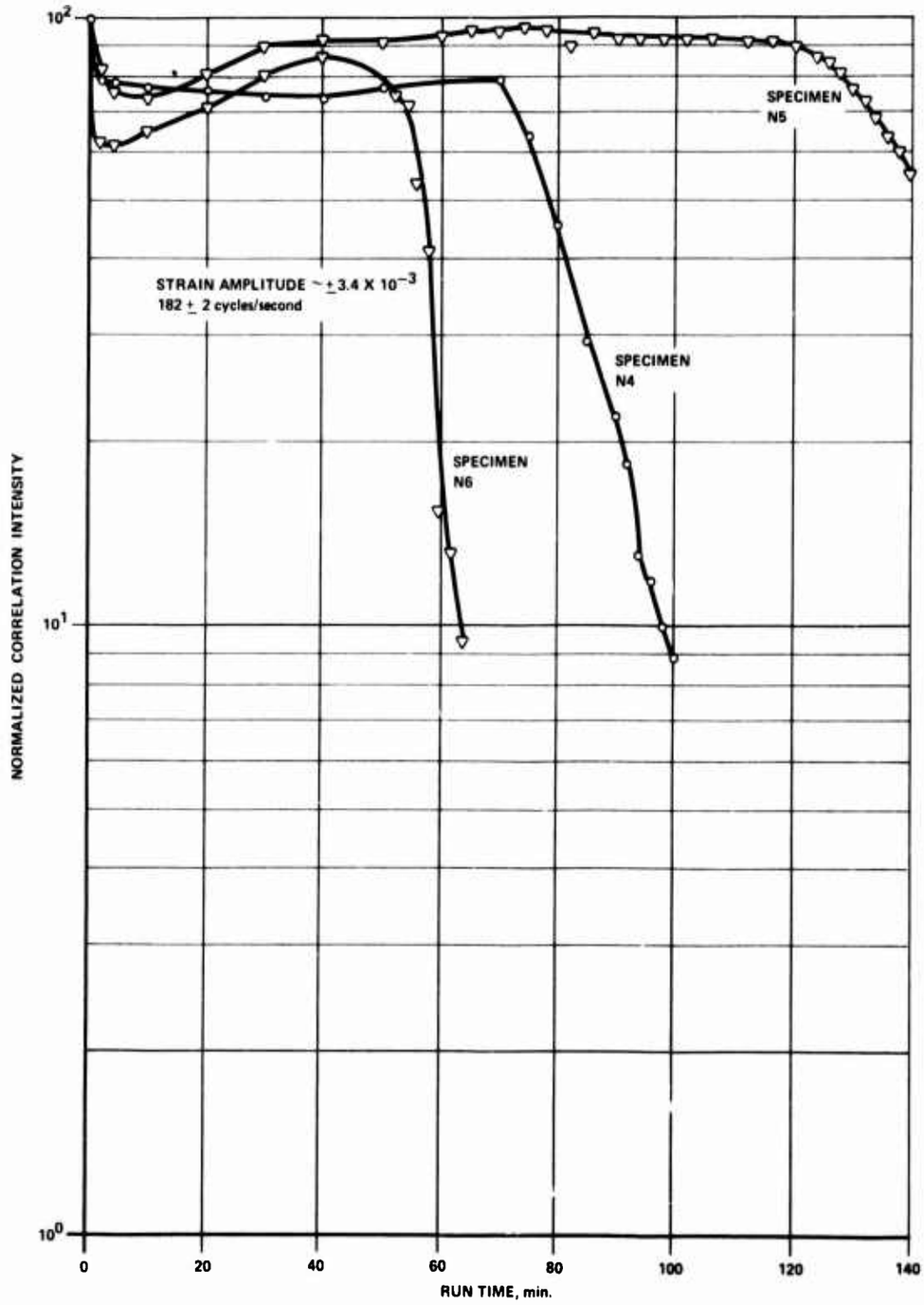

Figure 6. Correlation Intensity Versus Run Time for Specimens With Longitudinal Texture (Surfaces Finished With No. 600 Emery Paper).

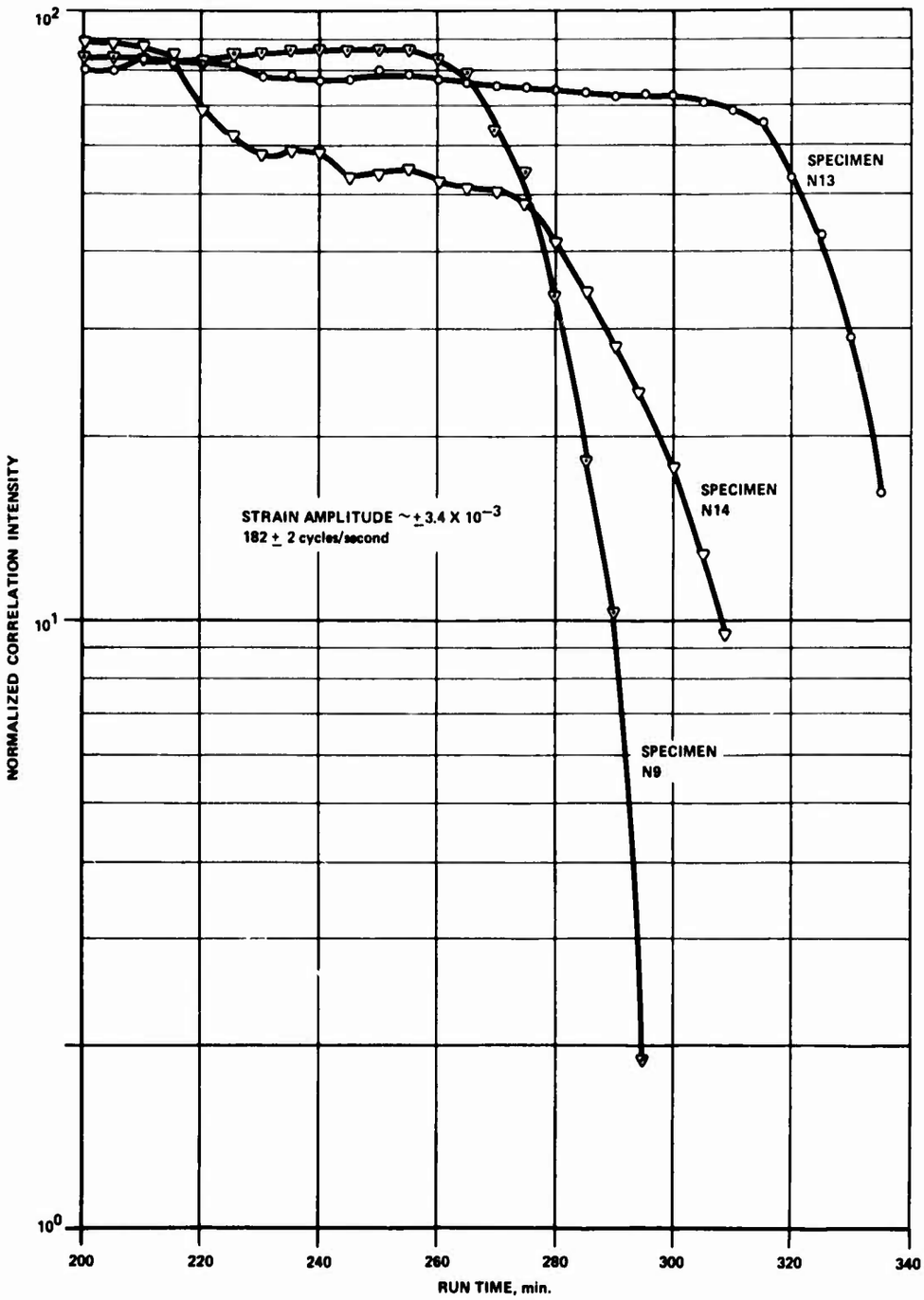

Figure 7. Correlation Intensity Versus Run Time for Specimens With Longitudinal Texture (Surfaces Finished With No. 600 Emery Paper).

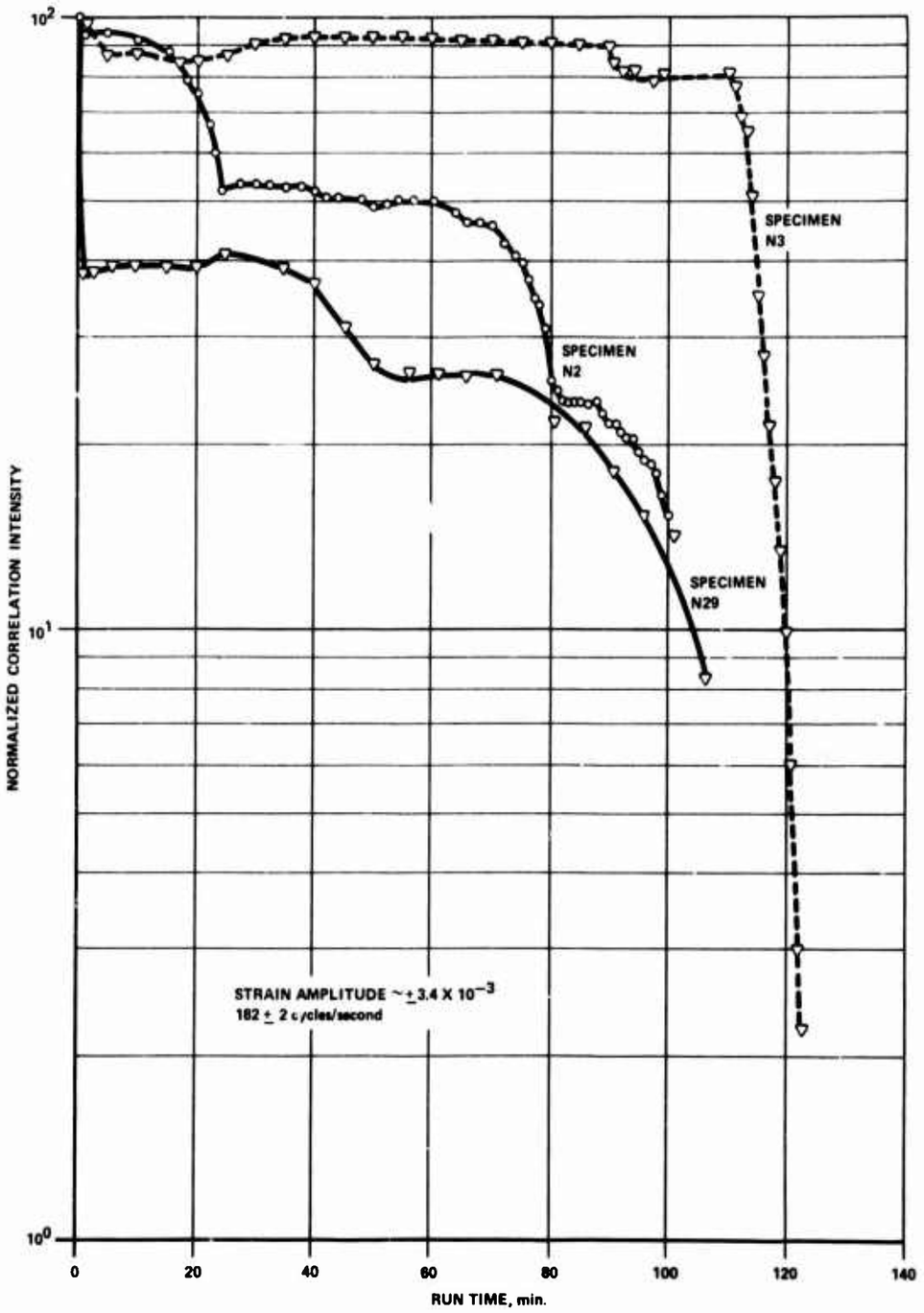

Figure 8. Correlation Intensity Versus Run Time for Specimens With Transverse Texture (As-Rolled Surfaces).

Figure 9. Effects of Stress Level on Fatigue Life.

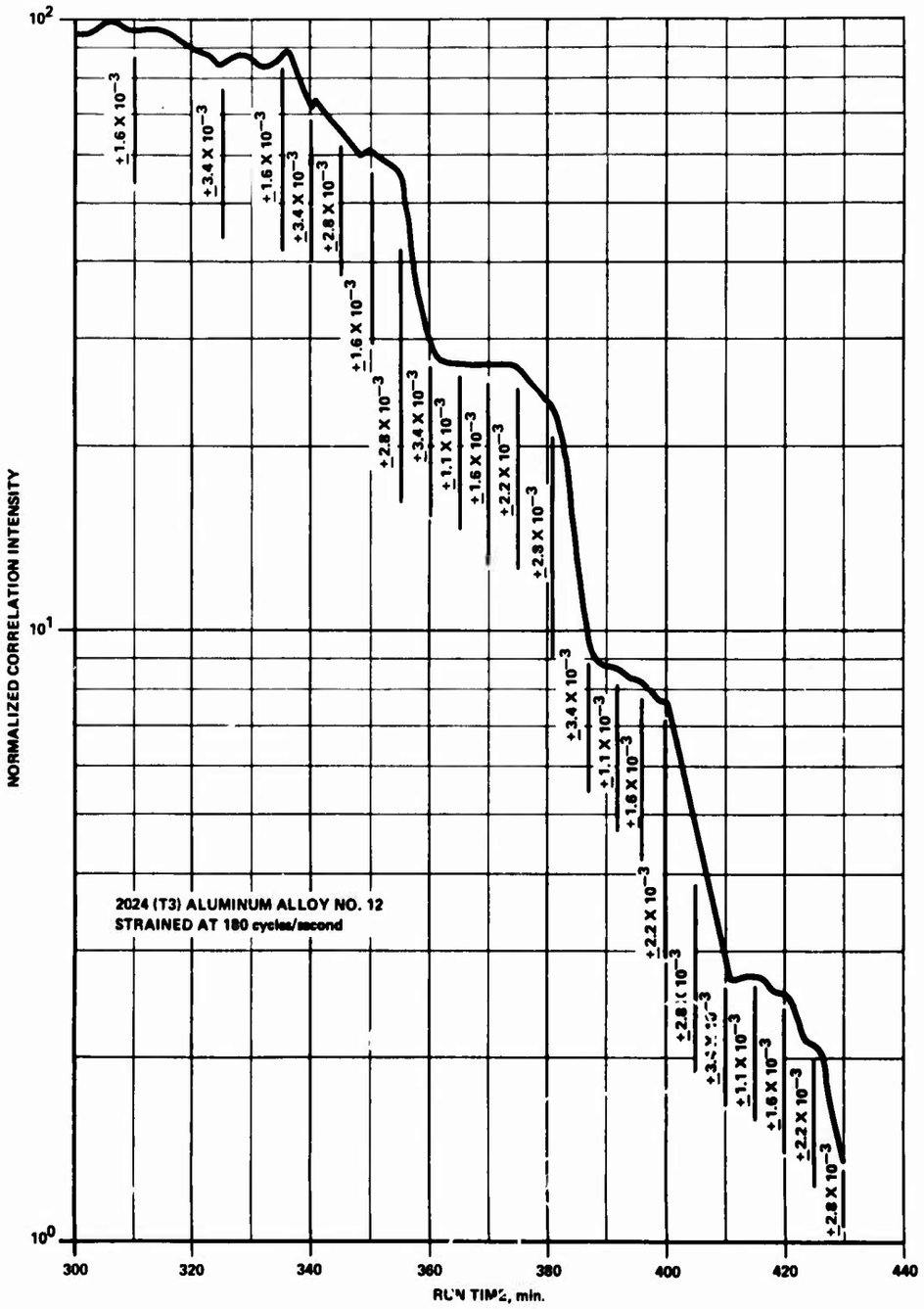

Figure 10. Effects of Stress Level on Stage III Decrease in the Correlation Intensity.

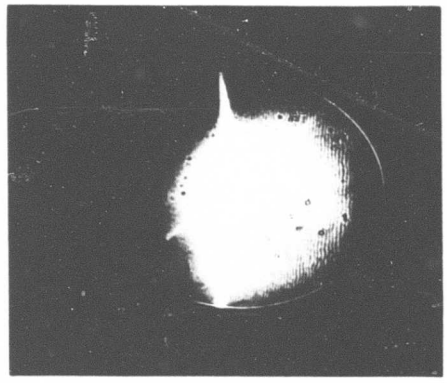

(a) As Received (Horizontal Scratches)

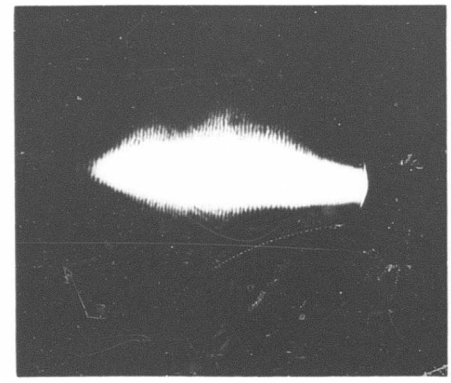

(b) No. 600 Emery Finish (Vertical Scratches)

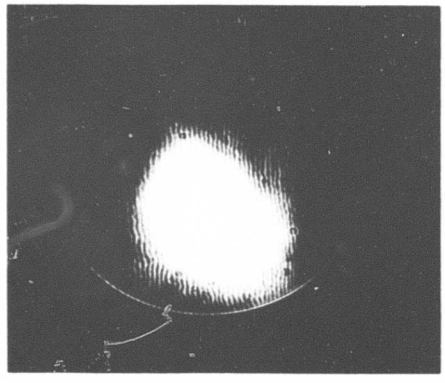

(c) No. 600 Emery Finish (Random Scratches)

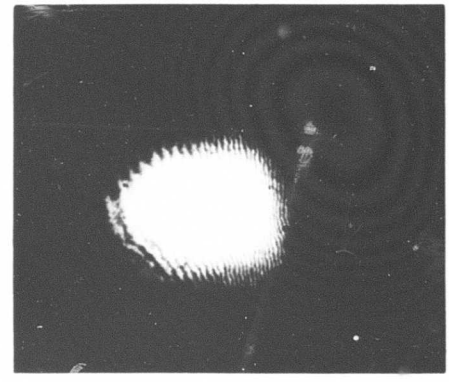

(d) Polished (No Scratches)

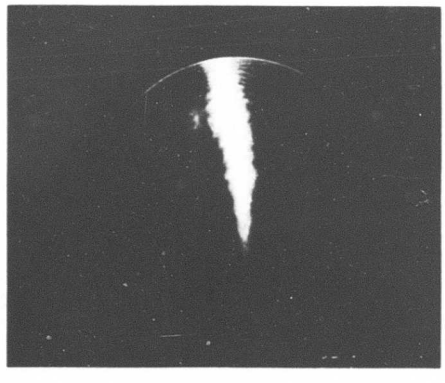

(e) Polished (Horizontal Scratches)

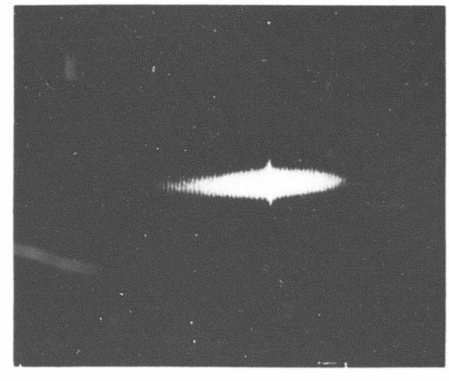

(f) Polished (Vertical Scratches)

Figure 11. Optical (Fourier) Spectra of Various Surface Finishes.

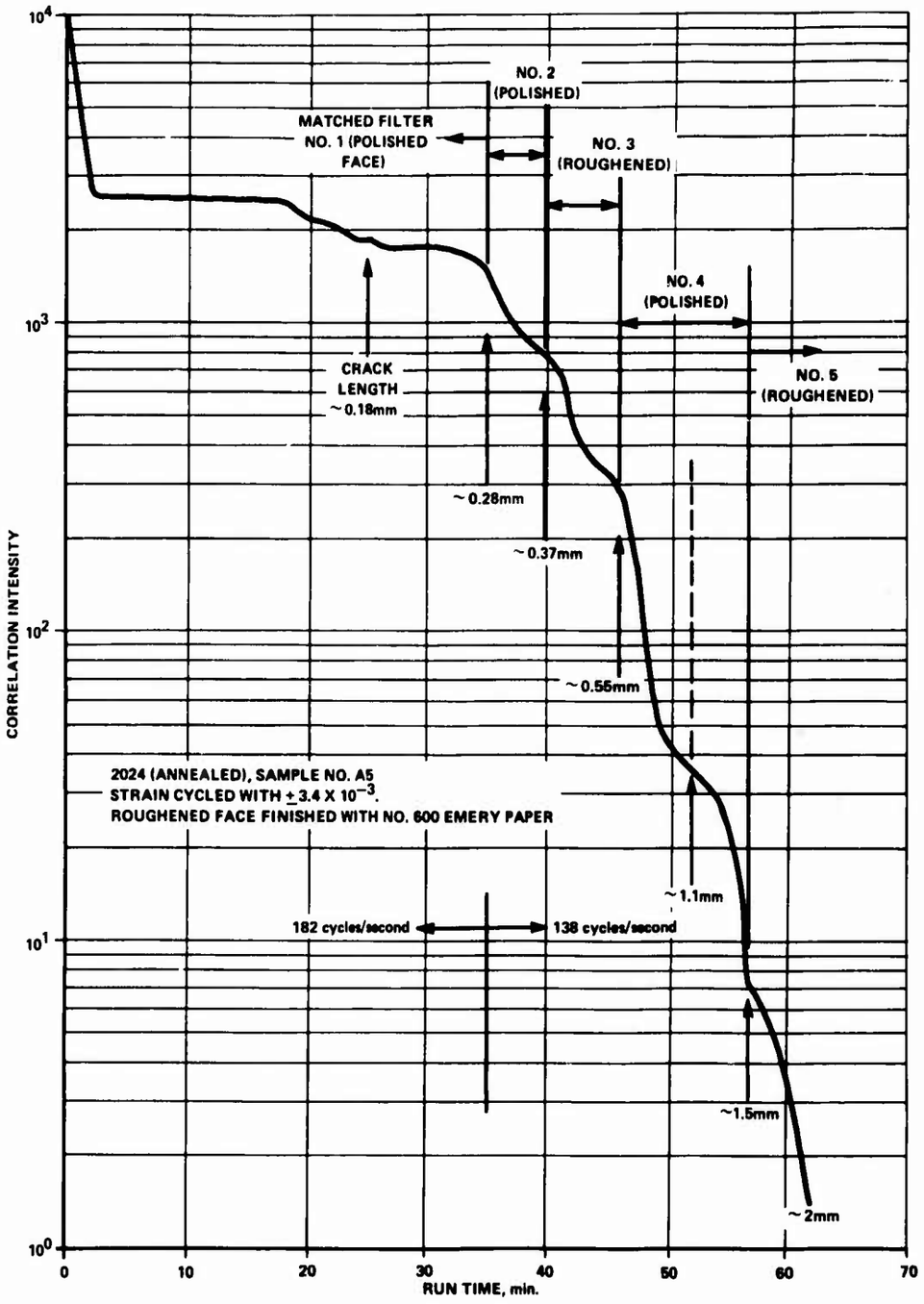

Figure 12. Effects of Surface Finish on Correlation Measurement.

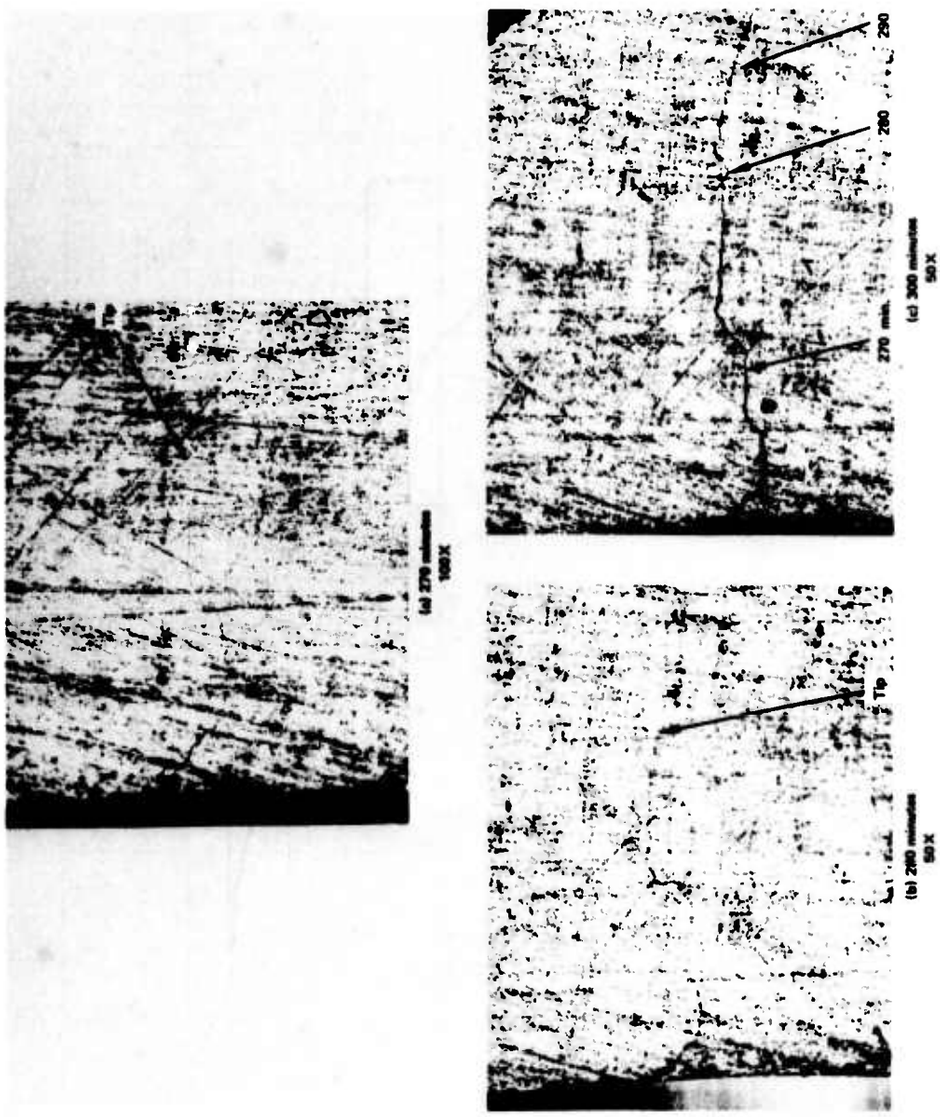

Figure 13. Photomicrographs Showing the Sequence of Crack Propagation in Specimen N9 Subjected to $\pm 3.4 \times 10^{-3}$ Strain Cycles (No. 600 Emery Paper - Random Scratches).

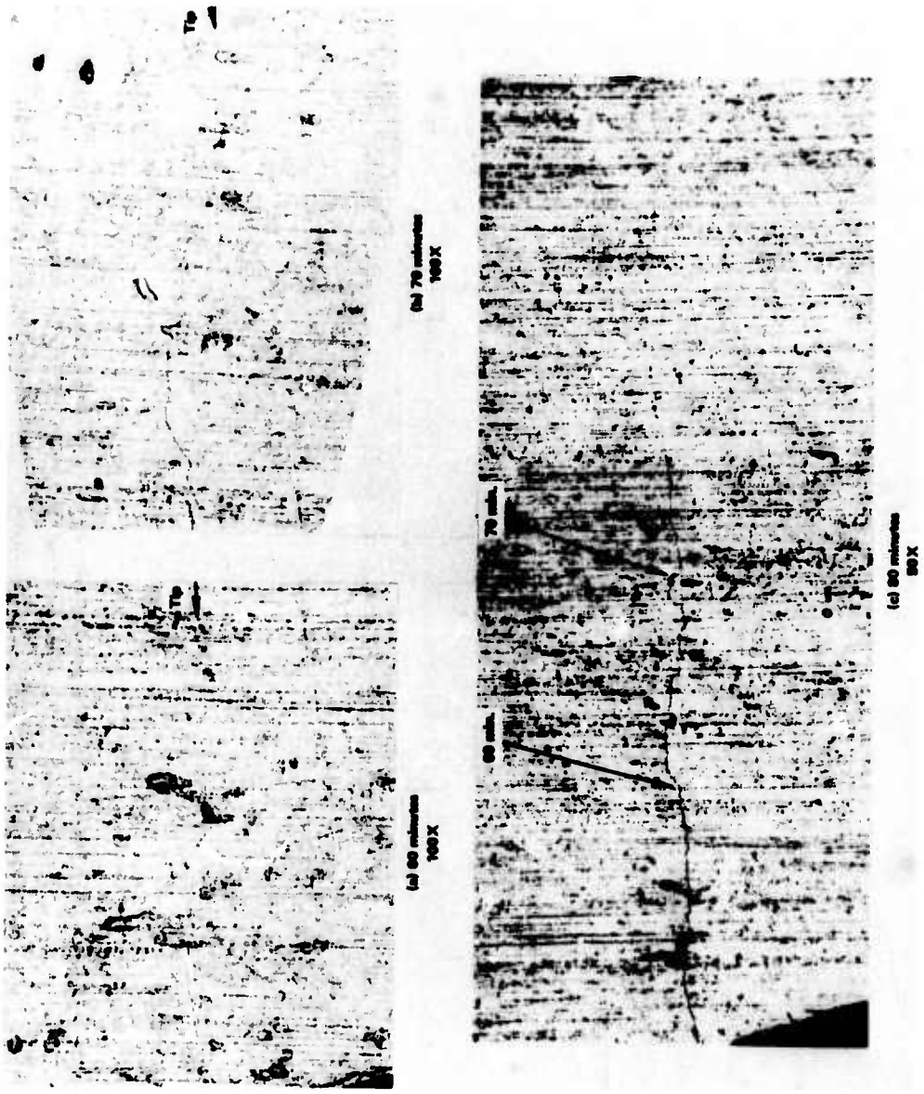

Figure 14. Photomicrographs Showing the Sequence of Crack Propagation in Specimen N11 Subjected to $\pm 3.4 \times 10^{-3}$ Strain Cycles (No. 600 Emery Paper - Random Scratches).

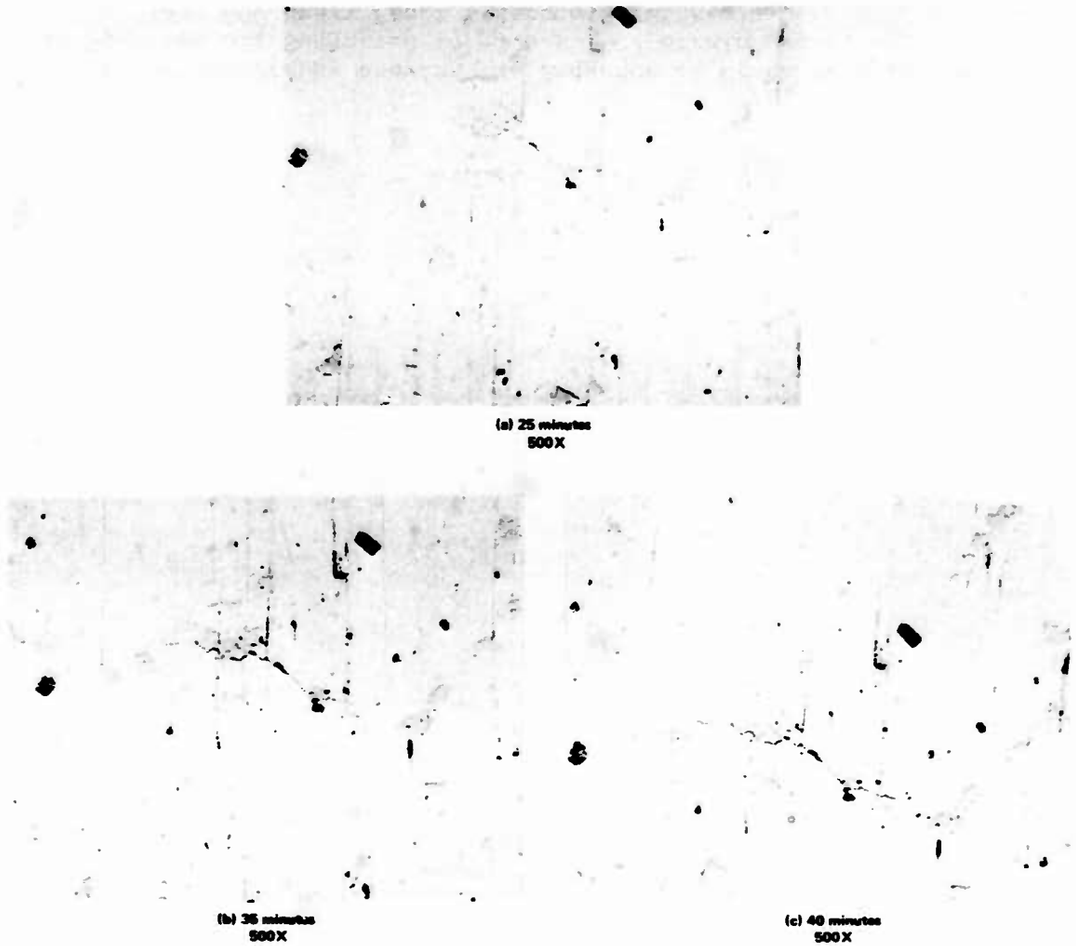

Figure 15. Photomicrographs Showing the Sequence of Crack Propagation in Specimen A5 Subjected to $\pm 3.4 \times 10^{-3}$ Strain Cycles (Annealed, Quenched, and Aged. Surface Chemically Polished).

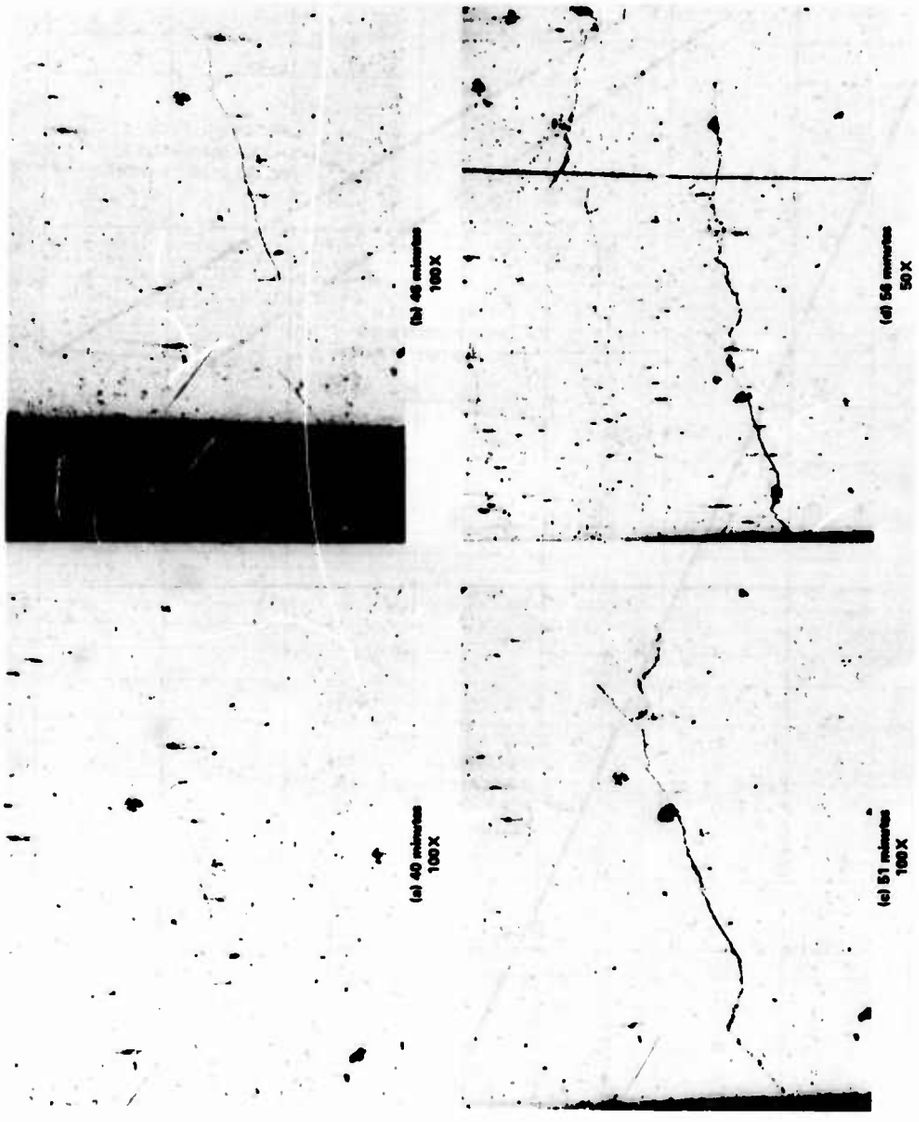

Figure 16. Photomicrographs Showing the Sequence of Crack Propagation in Specimen P5 Subjected to $\pm 3.4 \times 10^{-3}$ Strain Cycles (Polished Face).

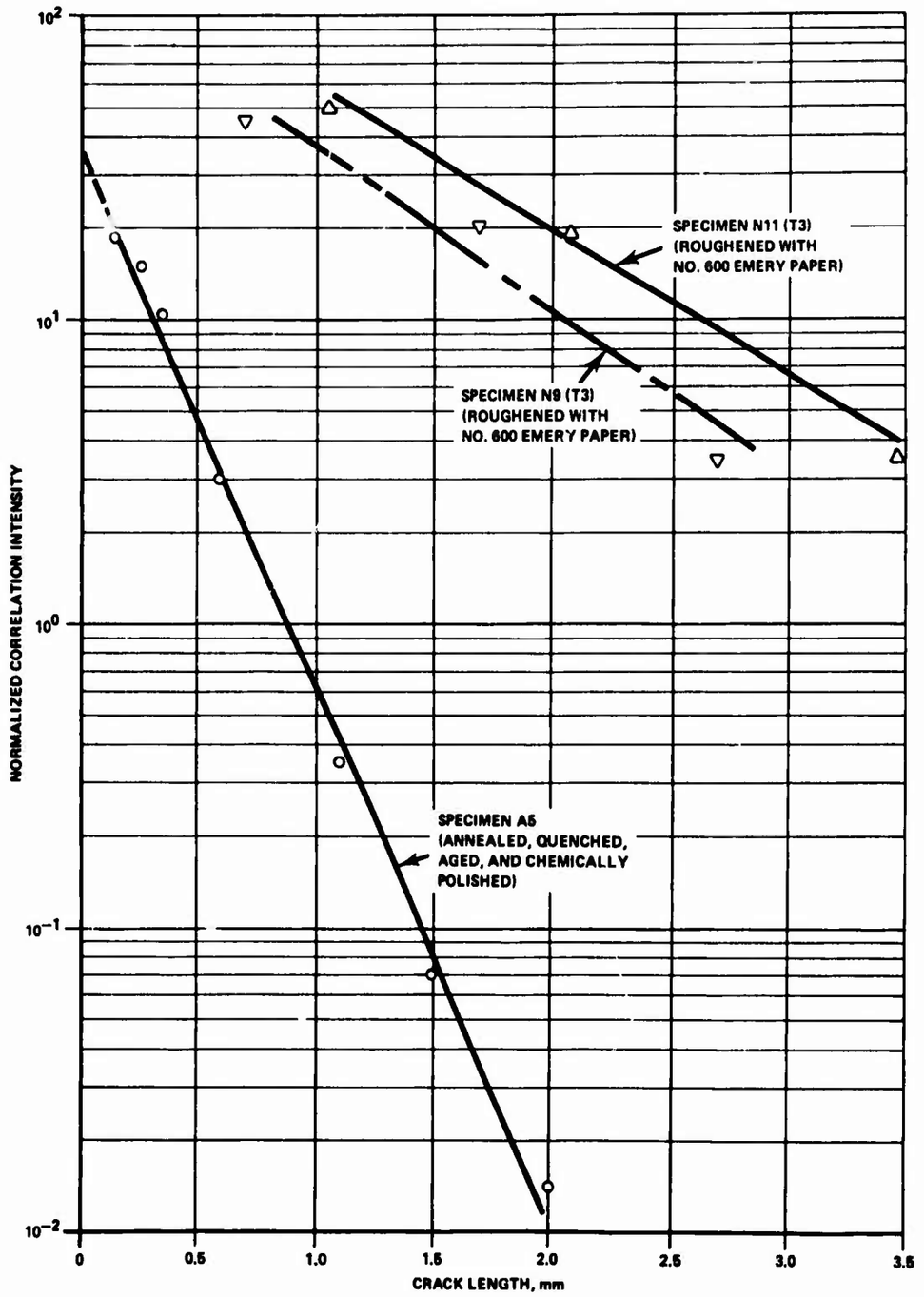

Figure 17. Correlation Intensity Versus Crack Length of Fatigued Specimens.

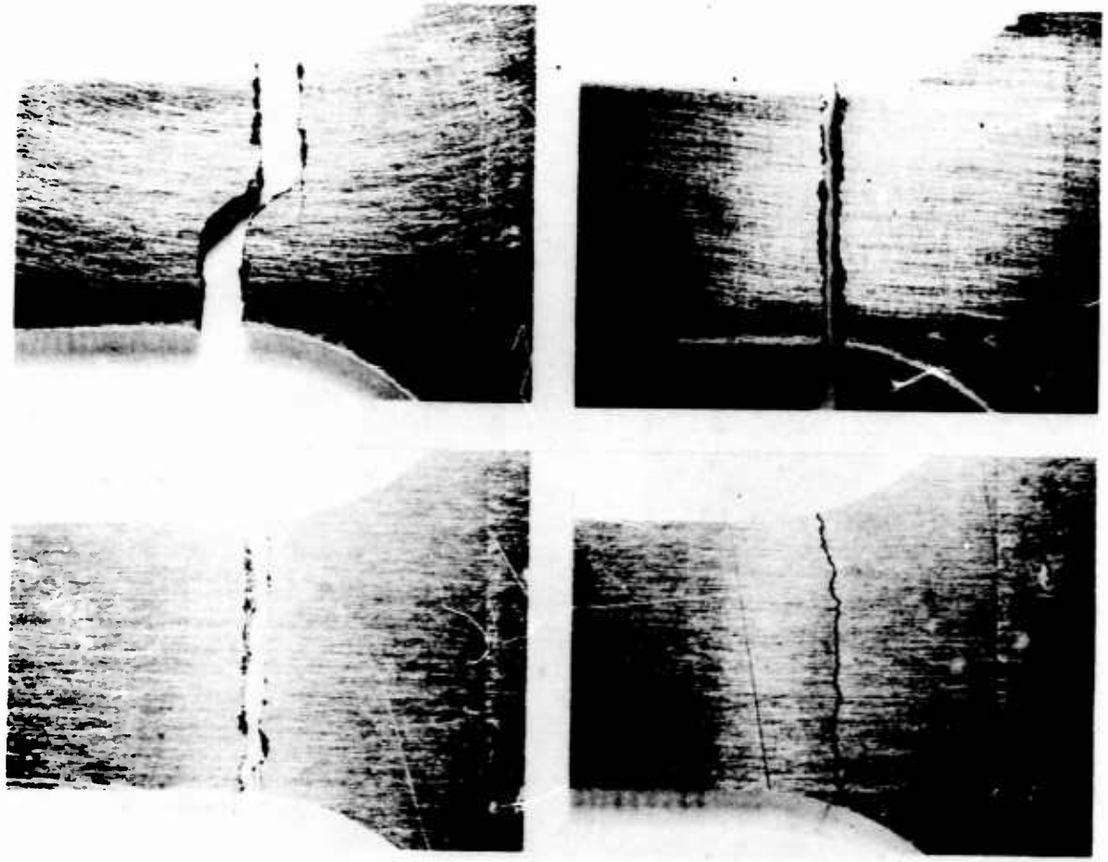

Figure 18. Failure Modes of Fatigued Specimens.

(a) Before Fatigue (Radiation Source Cu K_{α}. Film Distance 3.1 cm)

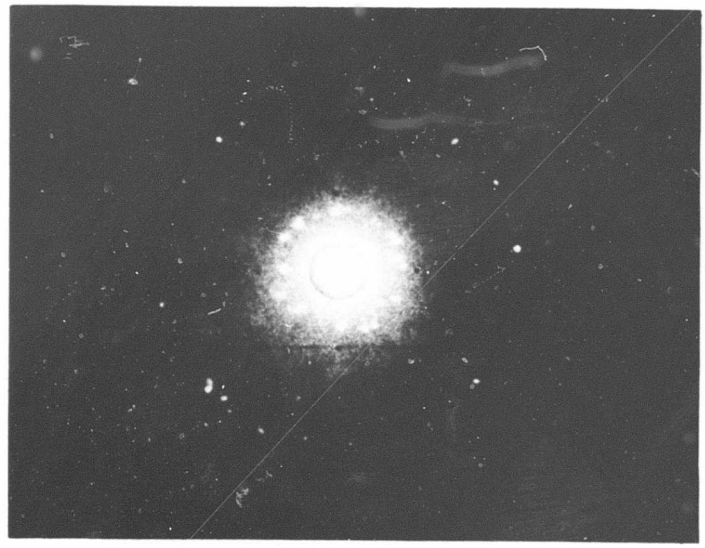

(b) Same Area as (a) After 5 Minutes (~55,000 Cycles) at a Strain Amplitude of $\pm 4 \times 10^{-3}$ (Radiation Source Cu K_{α}. Film Distance 3.1 cm)

Figure 19. X-Ray Laue Back Diffraction Photograph of the Critical Area of Specimen 114TA.

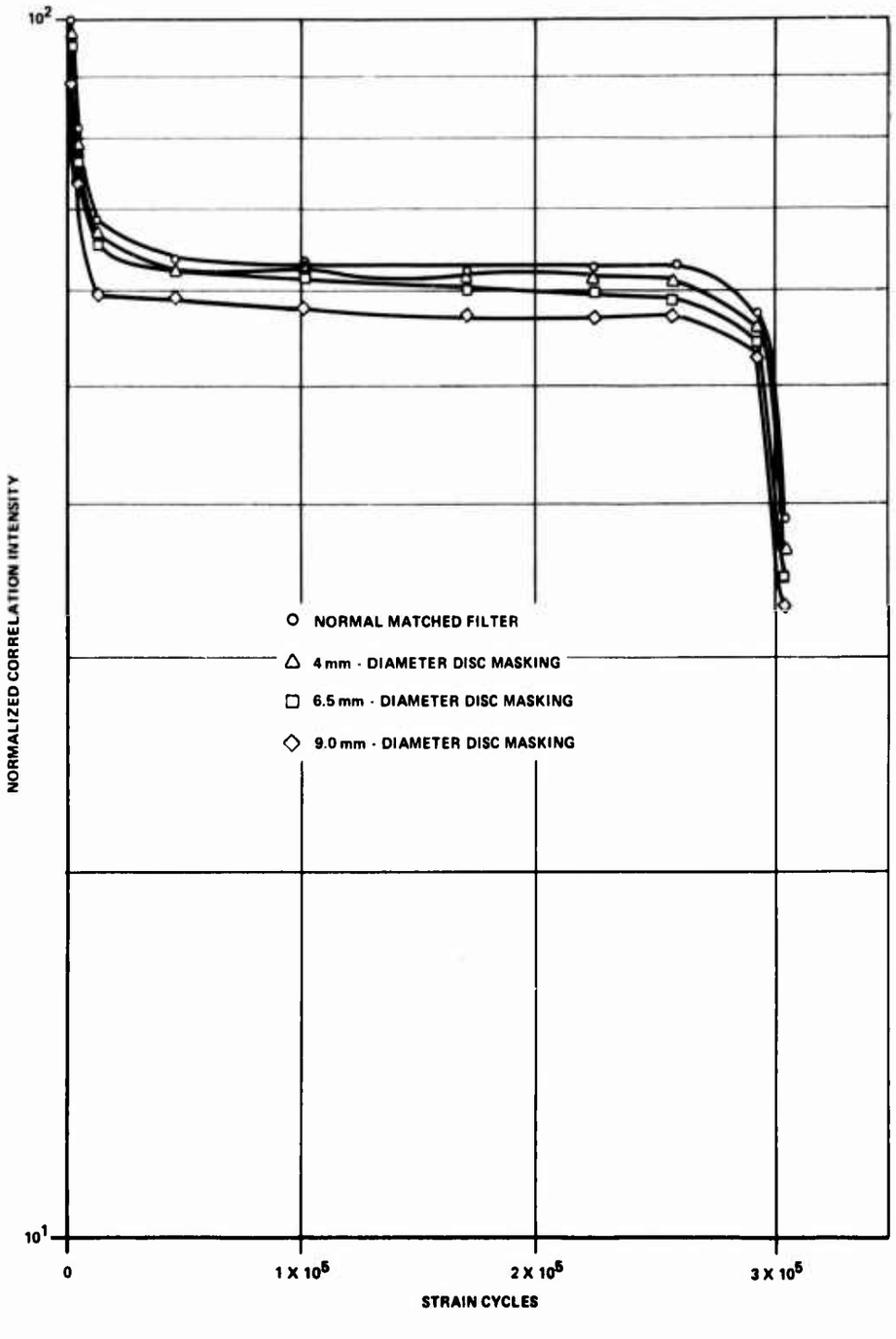

Figure 20. Correlation Measurements With Selective Masking of the Matched Filter in a Fatigue Test.

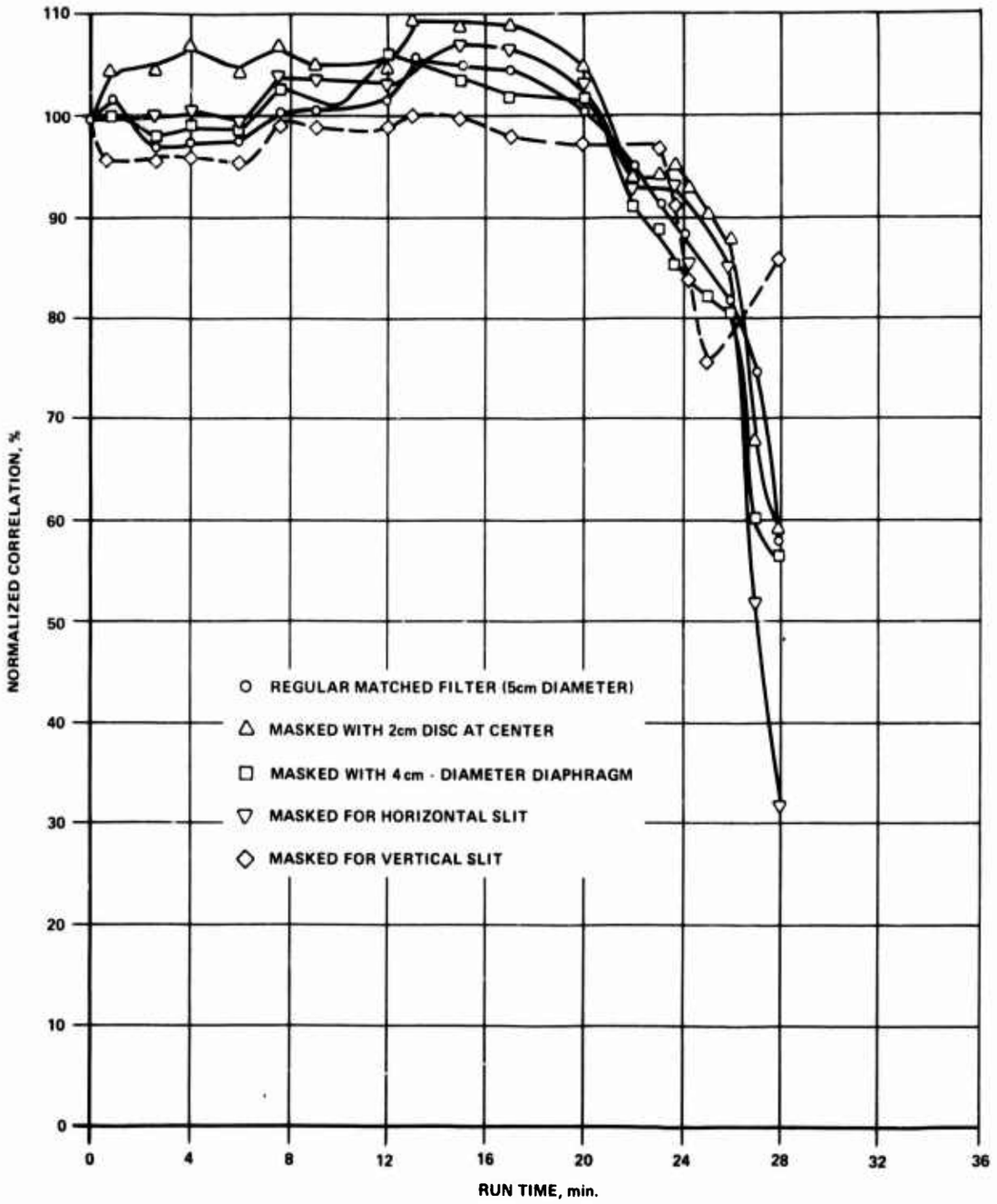

Figure 21. Correlation Measurements With Selective Masking of the Matched Filter in a Fatigue Test.

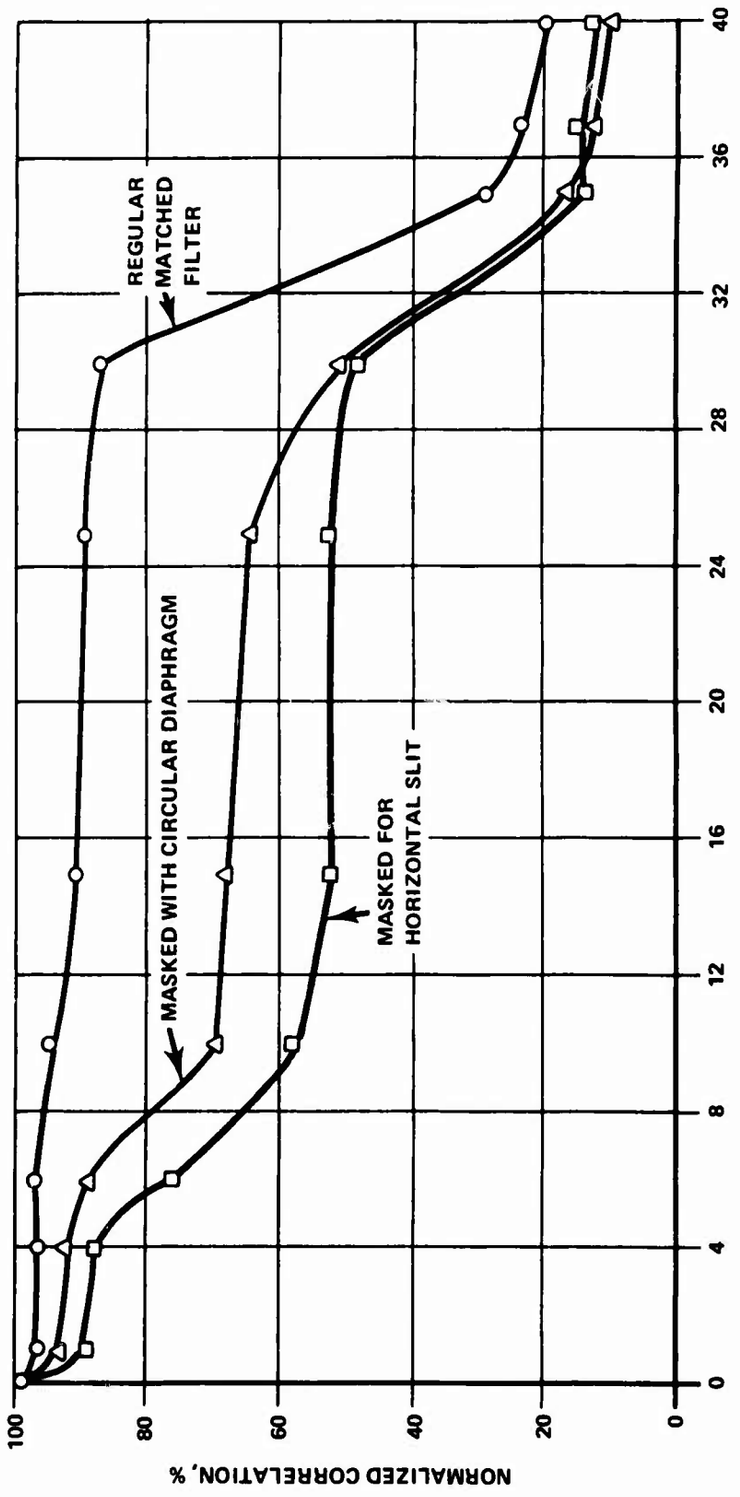

Figure 22. Correlation Measurements With Selective Masking of the Matched Filter in a Fatigue Test.

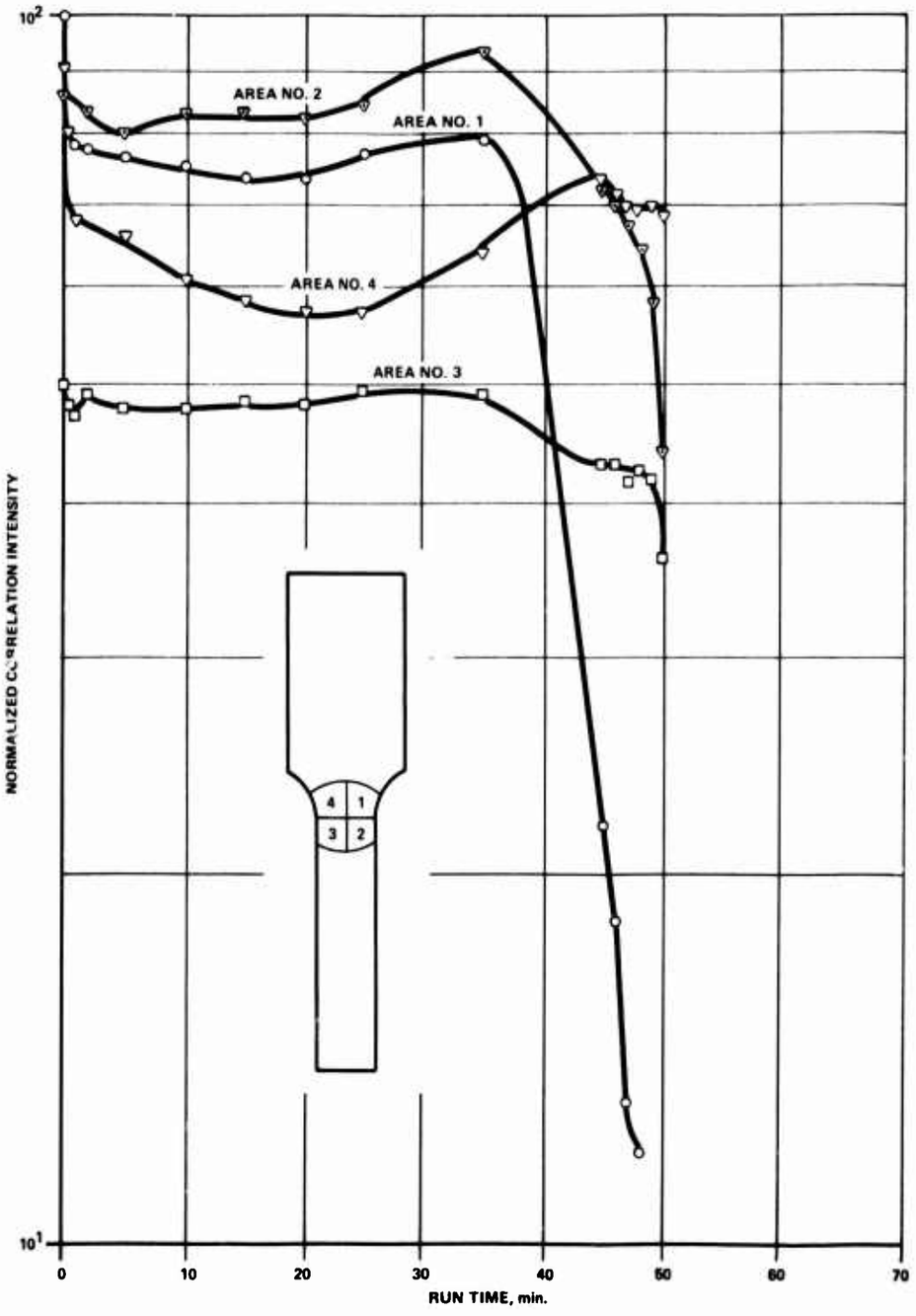

Figure 23. Correlation Intensity Versus Run Time Obtained by Selective Masking of the Specimen.

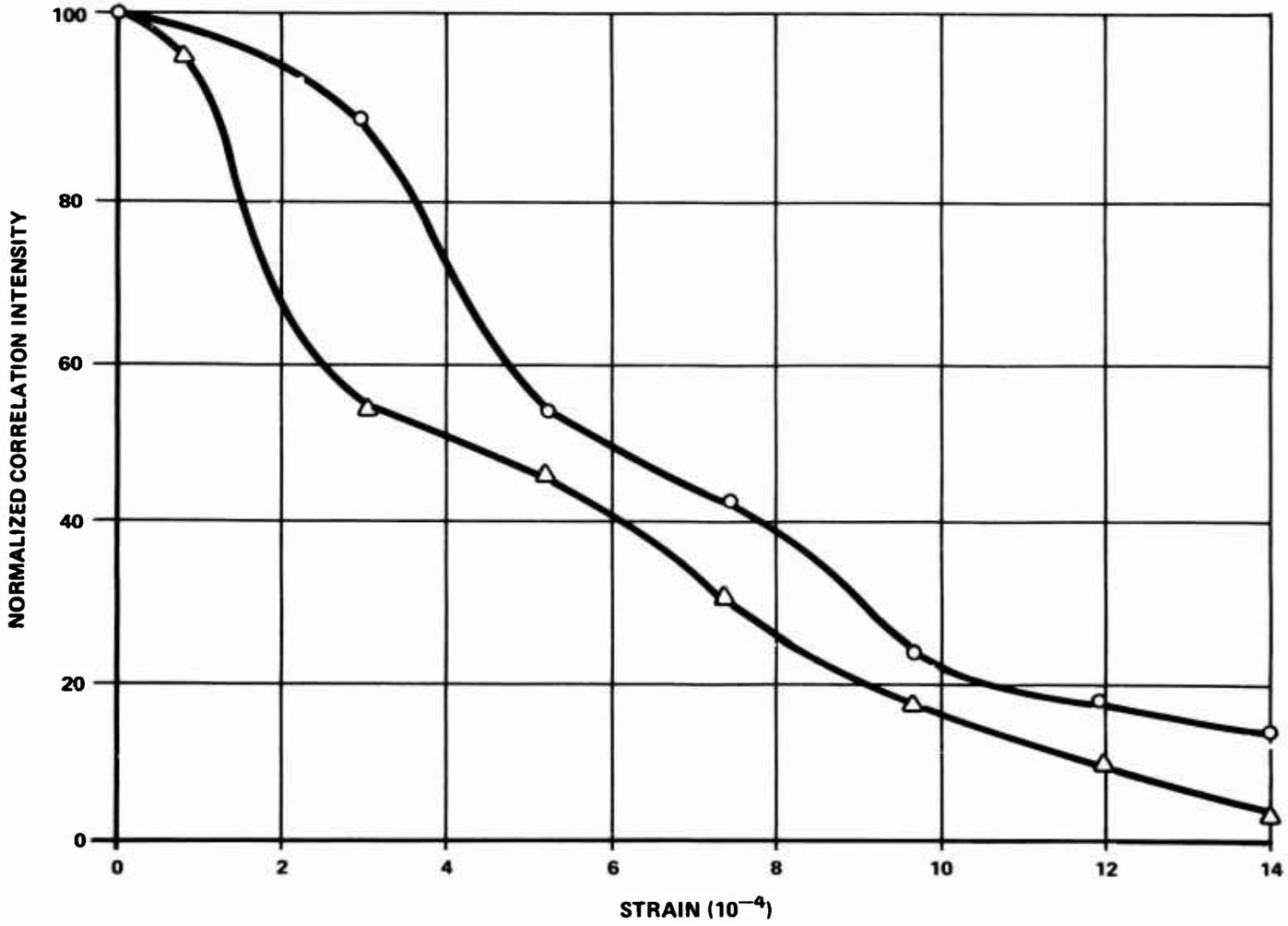

Figure 24. Correlation Intensity Versus Strain of Two Circular Areas Separated by a 1-Inch Distance.

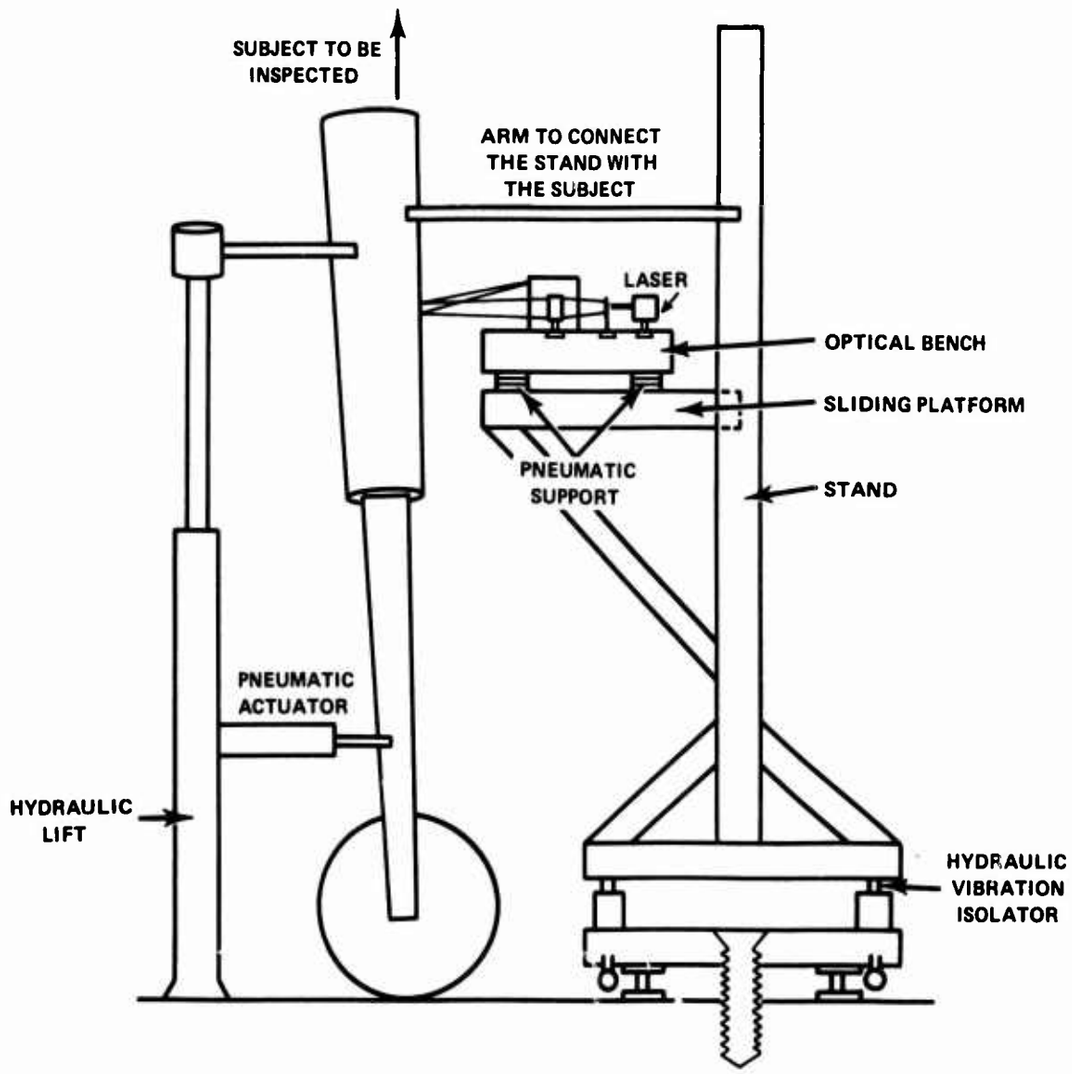

Figure 25. Prototype Field Inspection Instrument.

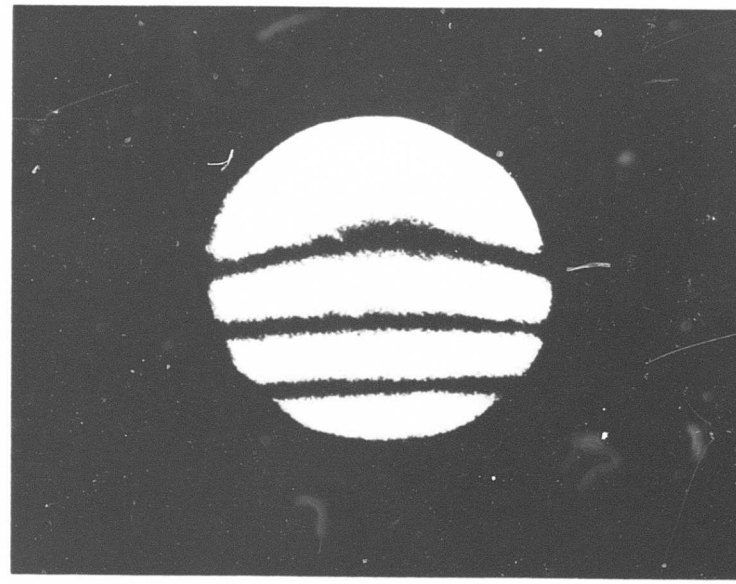

(a) T-Shaped Specimen
(Crack Propagating From Both Sides)

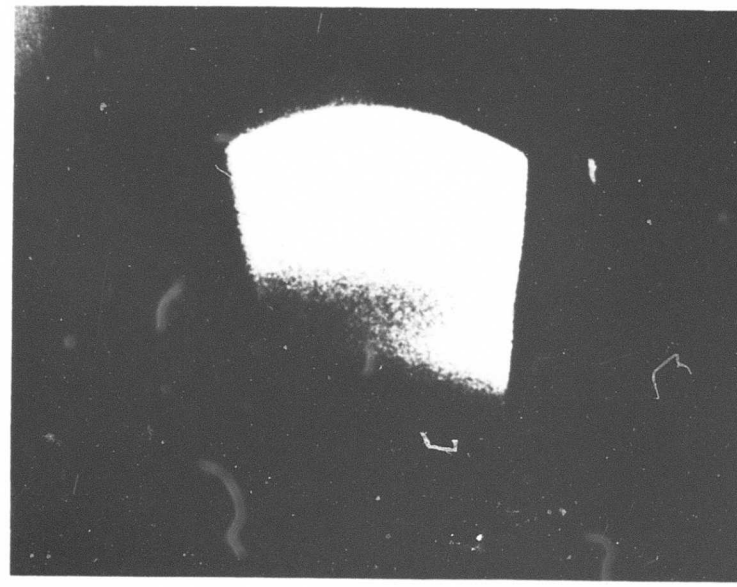

(b) Tapered Specimen
(Showing Bending of Specimen)

Figure 26. Holographic Interferograms Obtained With Double Exposure.

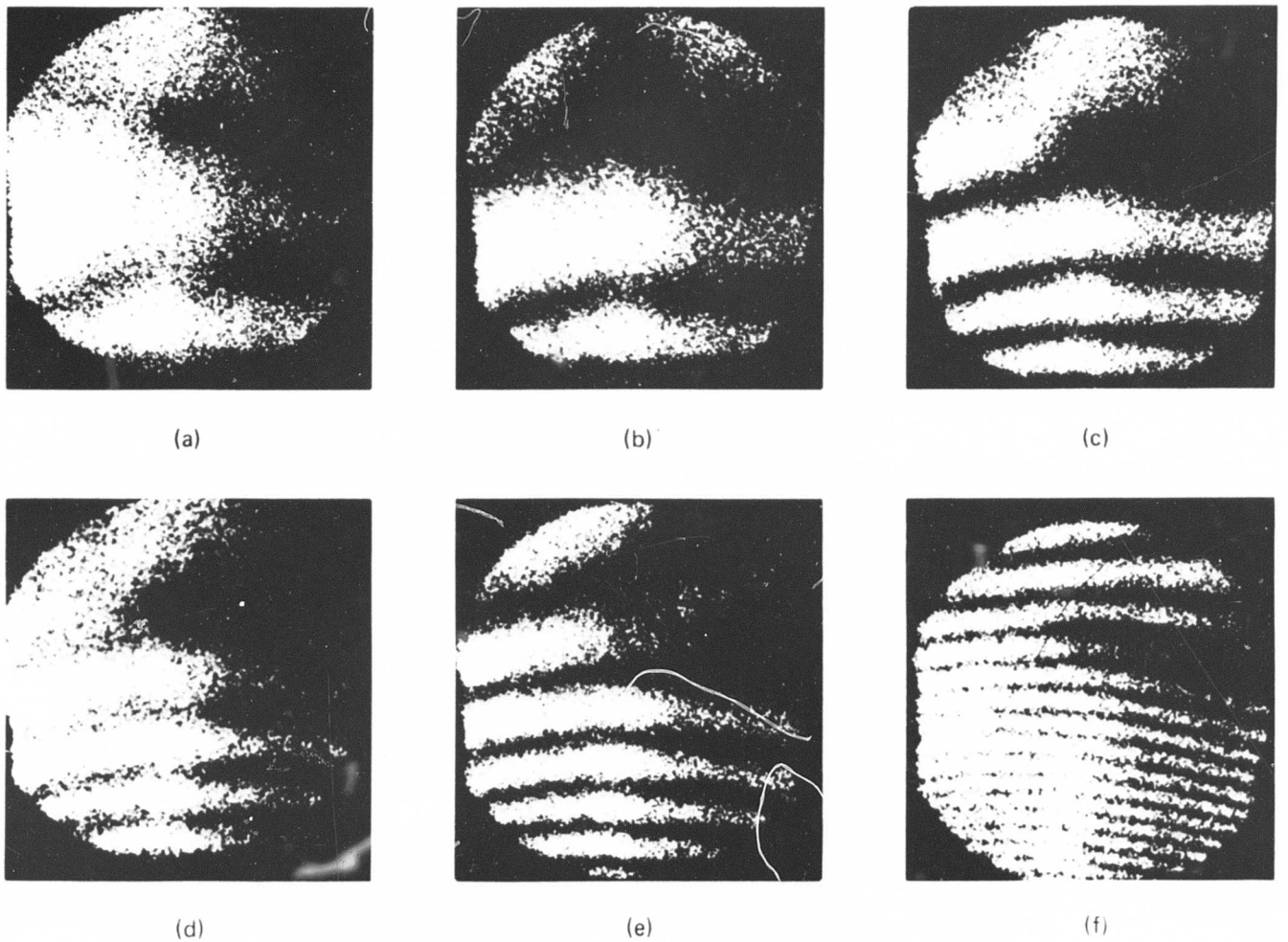

Figure 27. Holographic Interferometry Showing the Pattern When the Specimen Deforms in Bending.

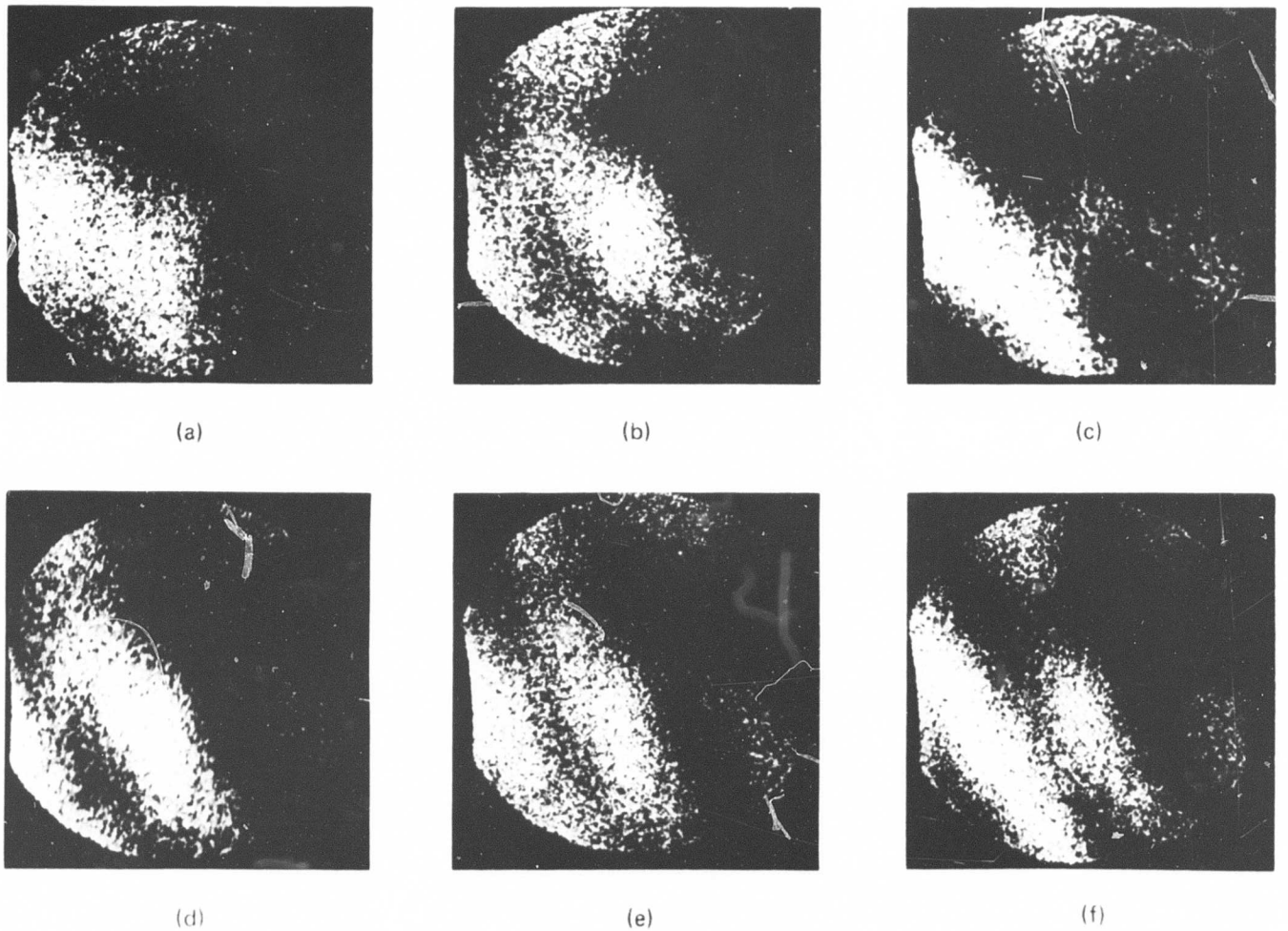

Figure 28. Holographic Interferometry Showing the Specimen Twisted.

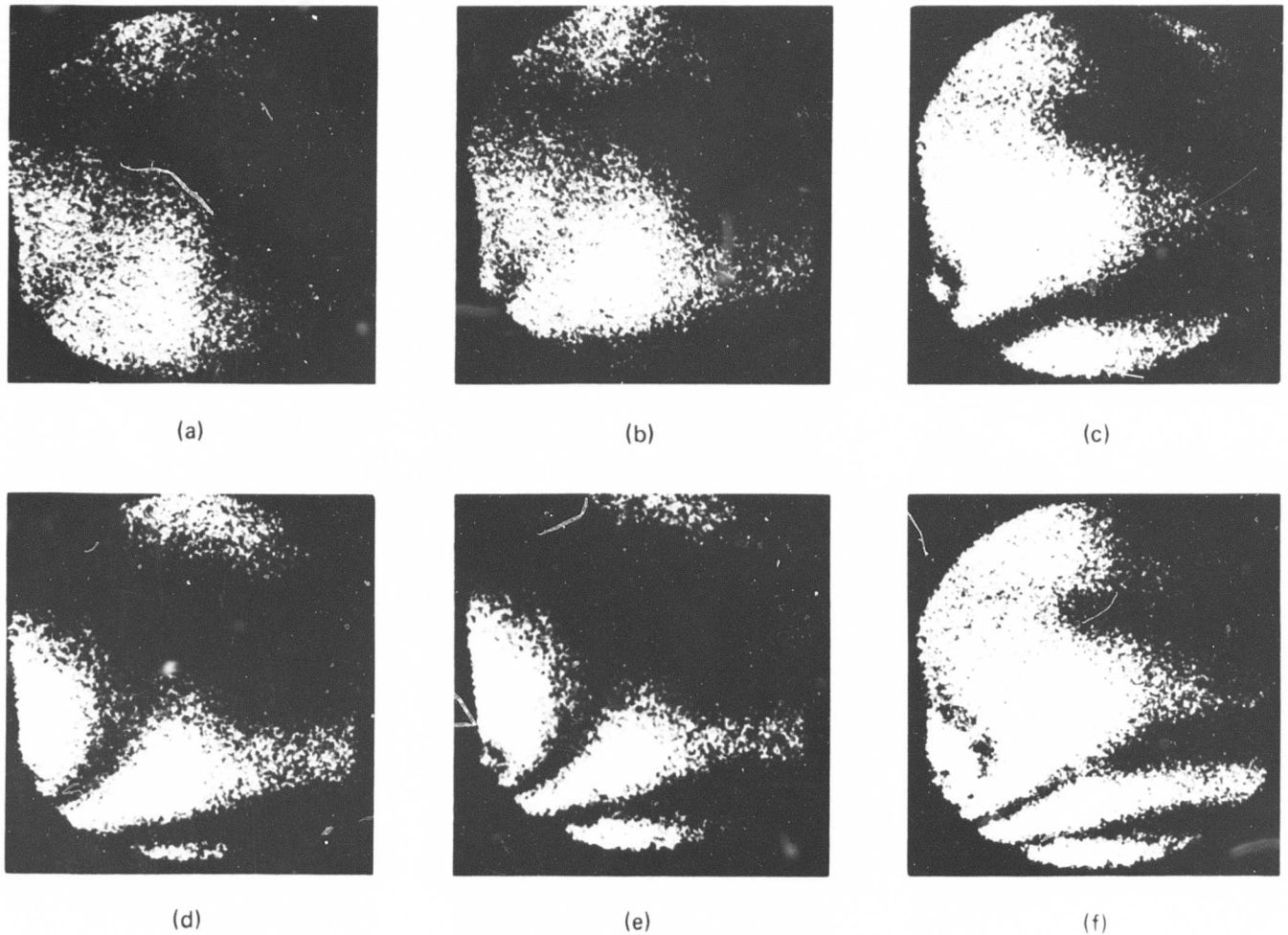

Figure 29. Holographic Interferometry Showing the Specimen Deformed.

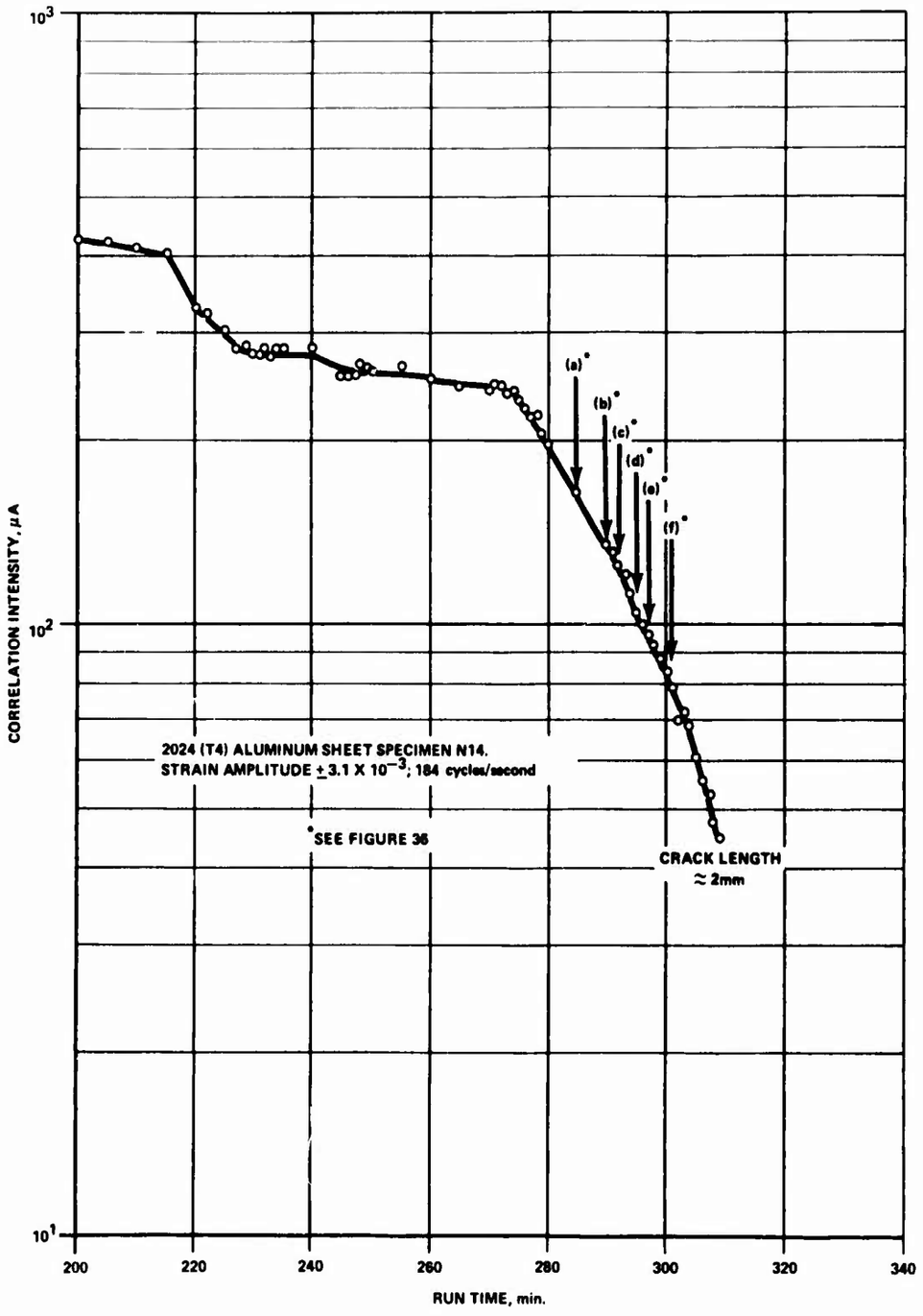

Figure 30. Correlation Intensity Versus Run Time Measured During Holographic Interferometry.

Unclassified

Security Classification

DOCUMENT CONTROL DATA - R & D

(Security classification of title, body of abstract and indexing annotation must be entered when the overall report is classified)

1. ORIGINATING ACTIVITY (Corporate author)	2a. REPORT SECURITY CLASSIFICATION
Bendix Research Laboratories 20800 10-1/2 Mile Road Southfield, Michigan	Unclassified 2b. GROUP

3. REPORT TITLE

FEASIBILITY OF USING OPTICAL CORRELATION TECHNIQUE FOR DETECTING IMPENDING FATIGUE FAILURE

4. DESCRIPTIVE NOTES (Type of report and inclusive dates)

Final Report 20 October 1967 to 20 October 1968

5. AUTHOR(S) (First name, middle initial, last name)

K. C. Chuang
E. Manuel Marom

6. REPORT DATE	7a. TOTAL NO. OF PAGES	7b. NO. OF REFS
April 1969	53	1

8a. CONTRACT OR GRANT NO.	9a. ORIGINATOR'S REPORT NUMBER(S)
DAAJ02-68-C-0024 b. PROJECT NO. Task No. 1F162203A43405 c. d.	USAAVLABS Technical Report 69-19 9b. OTHER REPORT NO(S) (Any other numbers that may be assigned this report) 4814 (BRL No.)

10. DISTRIBUTION STATEMENT

This document has been approved for public release and sale; its distribution is unlimited.

11. SUPPLEMENTARY NOTES	12. SPONSORING MILITARY ACTIVITY
	US Army Aviation Materiel Laboratories Fort Eustis, Virginia

13. ABSTRACT

An investigation to determine the feasibility of using an optical correlation technique to detect fatigue cracks in materials is discussed. The optical system used included a helium-neon gas laser for generating coherent light, a commercially available photographic plate for recording the hologram, and a photomultiplier tube for measuring the light intensity. As a part of the investigation, holographic interferometric experiments were performed for comparison. During testing, aluminum-alloy specimens with various surface finishes and configurations were subjected to different stress levels and the effects were measured. Results indicated that the optical correlation technique is capable of detecting cracks as small as 0.05 mm in length and can detect even smaller dimensions in width and depth, although in practice 1 mm in length is the resolution limited by the instrumentation. In comparison, the resolution of the holographic interferometric technique was found to be limited to the width of the specimen, making it less sensitive in detecting surface deformation. The sensitivity of neither method was affected by surface finish, stress level, or specimen configuration.

DD FORM 1 NOV 68 1473 REPLACES DD FORM 1473, 1 JAN 64, WHICH IS OBSOLETE FOR ARMY USE.

Unclassified

Security Classification

14. KEY WORDS	LINK A		LINK B		LINK C	
	ROLE	WT	ROLE	WT	ROLE	WT
Optical Correlation Technique Detecting Fatigue Failure Laser Holographic Interferometry Crack Propagation						

3783-69

END